Review of Palaeobotany and Palynology 276 (2020) 104205

Contents lists available at ScienceDirect

Review of Palaeobotany and Palynology

journal homepage: www.elsevier.com/locate/revpalbo

Paleoecological archives unraveling the early land-use history at the emergence of the Bronze Age settlement of Bergamo (Italian Alps)

Cesare Ravazzi [a,*], Roberta Pini [a], Mattia De Amicis [b], Lorenzo Castellano [c], Roberto Comolli [b], Davide Abu El Khair [b], Giulia Furlanetto [b], Diego Marsetti [d], Renata Perego [a]

[a] Research Group on Vegetation, Climate and Human Stratigraphy, Lab. of Palynology and Palaeoecology, CNR-IGAG, Piazza della Scienza 1, 20126 Milano, Italy
[b] Dept. of Environmental and Earth Sciences, University of Milano-Bicocca, Piazza della Scienza 1, 20126 Milano, Italy
[c] New York University, Institute for the Study of the Ancient World, East 84th Street, New York, USA
[d] ECOGEO srl, via Fratelli Calvi 2, 24122 Bergamo, Italy

ARTICLE INFO

Article history:
Received 12 February 2020
Accepted 28 February 2020
Available online 02 March 2020

Keywords:
Vegetation history
Cultural landscape
Pastures
Livestock watering
Phosphorus
Bronze Age

ABSTRACT

The hilltop town of Bergamo, at the southern fringe of the Italian Alps, represents a typical example of the stepped emergence of a prehistoric settlement developing into a proto-historic urban center in the Iron Age. We present here unprecedented multidisciplinary evidence based on several near-site stratigraphies, supported by a robust radiocarbon chronology and by a continuous fine-resolution sedimentary and paleoecological record from a pond used for livestock watering, which was intercepted by drilling underneath the modern Catholic Cathedral. The obtained chronostratigraphy documents the development of arable and fallow land including cereals, legumes and livestock husbandry starting as early as 3355 yrs. cal BP (median of modeled calibrated ages, i.e., 15th century BC). This evidence indicates that already in the Middle Bronze Age the very center of the hilltop of the Bergamo Hill supported an early farming center. Land use reached an acme between 2980 and 2753 yrs. cal BP, triggering intense soil erosion by runoff processes. Paleobotanical evidence suggests uphill grapevine cultivation at the southern Alpine fringe at 2900 yrs. cal BP. Data support settlement continuity until around 2700 yrs. cal BP (8th century BC), before the growth of the Celtic town in the 6th–5th century BC. The location and development of the farming center yet in the Bronze Age might have been promoted by topographical diversification, high geomorphic weathering rate, soil suitability for agriculture and pastoralism, and water availability on the northern side of the hill, secured by orographic precipitation in warmer seasons.

1. Introduction

In several regions of Europe, including N-Italy, the emergence of urban centers is regarded as a distinctive phenomenon of the Iron Age (Sievers and Schönfelder, 2012; Fernández-Götz, 2015). This first appearance and development of urban centers represents a well-known watershed in protohistory, bearing far-reaching direct repercussions on both modality and scale of interaction between human communities and their natural surroundings and forcings. Besides proving several research opportunities, the highly anthropized landscapes resulting from those dynamics pose a new set of challenges to archeology and Quaternary paleoecology. In fact, the increased complexity in the systemic relationship between natural and anthropic processes translates in an intricated meshwork of feedbacks between culture, economy, land-use, vegetation, and climate, which disentanglement is intrinsically problematic. In order to shed light on those crucial processes, multiproxies paleoenvironmental records directly associable to those early urban centers are needed.

Excellent, though indirect, sedimentary records are often available off-site to settled hills, such as footslope lacustrine and fluviatile environments (Ledger et al., 2015), harbors (Ravazzi et al., 2013; Sadori et al., 2015) and Mediterranean bays and coastal lagoons (Morellón et al., 2016). On the other hand, however, paleoenvironmental archives directly associated with those early urban centers buried underneath modern cities are systematically overlooked, due to low visibility and difficult accessibility to urban stratigraphies. In the past decades, our knowledge of urban archeological deposits drastically increased, thanks to regulations of underground construction activities, often involving archeological monitoring and development-led excavation projects. In this framework, however, natural archives are often disregarded, simply because archeological digging ends when there is no macroscopic sign of occupation (Barker, 1993), regardless the potential of detecting agropastoral activities, reconstructing past environments, and

* Corresponding author.
E-mail addresses: cesare.ravazzi@cnr.it, cesare.ravazzi@cnr.it (C. Ravazzi), roberta.pini@igag.cnr.it (R. Pini), mattia.deamicis@unimib.it (M. De Amicis), lc2995@nyu.edu (L. Castellano), roberto.comolli@unimib.it (R. Comolli), davide.abuelkhair@gmail.com (D.A. El Khair), g.furlanetto1@campus.unimib.it (G. Furlanetto), diego.marsetti@ecogeo.net (D. Marsetti), renaperego1@gmail.com (R. Perego).

https://doi.org/10.1016/j.revpalbo.2020.104205
0034-6667/

predicting near-site to settlements through microbotanical evidence (Edwards, 1991; Mercuri et al., 2014; Ravazzi et al., 2019).

While buried urban structures can often be located and identified through geophysical prospections and remote sensing (Ninfo et al., 2009), the more ephemeral evidence of agropastoral activities hidden under a thick pile of urban deposits can be easily reached by drilling, remaining otherwise inaccessible to research. Thus, the study of high resolution near-site drilling stratigraphies, combining and integrating microbotanical data with sedimentary and radiocarbon evidence, is a strategy of far-reaching applicability to the study of the early history of urban centers, especially in terms of settlement continuity before the presumed foundation of an urban center itself. Furthermore, multidisciplinary paleoecology allows to detect phases of contraction and intensification of land-use, and to relate them to coeval changes in climate, demographic, or socio-economic systems. Independent climate proxies, such as glacier advances (Le Roy et al., 2015), isotopic records (Fohlmeister et al., 2013), and quantitative reconstructions from high-altitude dendrochronology and pollen records (Nicolussi et al., 2005; Furlanetto et al., 2018) are now available for most of the Holocene in the Alpine region, thus potentially allowing to disentangle the anthropogenic signal from climate forcing (Tinner et al., 2003).

As part of this broader inquiry on the environmental context of the origin and earliest history of European modern cities, we present here the multidisciplinary stratigraphic record obtained from drillings and archeological trenches underlying the modern city of Bergamo (45°42′14″ N, 9°39′46″ E), on top of the homonymous hill at the Italian Alpine fringe (Fig. 1). Below the archeological layers, we explored natural deposits rich in botanical remains which turned out to testify the emergence of an early settlement dated to the Late (i.e., 1300–1100 yrs. cal BC in N-Italy, De Marinis, 2014) to Final Bronze Age (i.e. 1100–900 yrs. cal BC), followed by the development of the urban center in the Iron Age. Cultural and climate constrains will be discussed.

2. The development of the ancient city at the hilltop of Bergamo

The history of the ancient city on the hilltop of Bergamo (*Città Alta*), at the southern fringe of the Italian Alps in Lombardy (Fig. 1), is a well-known example of hilltop settlement founded in protohistoric times by Celtic groups belonging to the Golasecca archeological cultural complex (Poggiani Keller, 2007). The Celtic settlement will eventually develop by the late 2nd–early 1st century BC into the monumental Roman town of *Bergomum* (Fortunati, 2012). The monumental development of the ancient city of Bergamo culminates with the construction its medieval basilica, the *Cappella Colleoni*, a masterwork of Renaissance architecture, and the defense walls built by the Republic of Venice in the 16th century (Fig. 1c and 2).

Archeological evidence points to the rise of an urban center on the hilltop of Bergamo around 500 BC, a period corresponding to the cultural phase of Golasecca II B (Poggiani Keller, 2001). In the 6th–5th

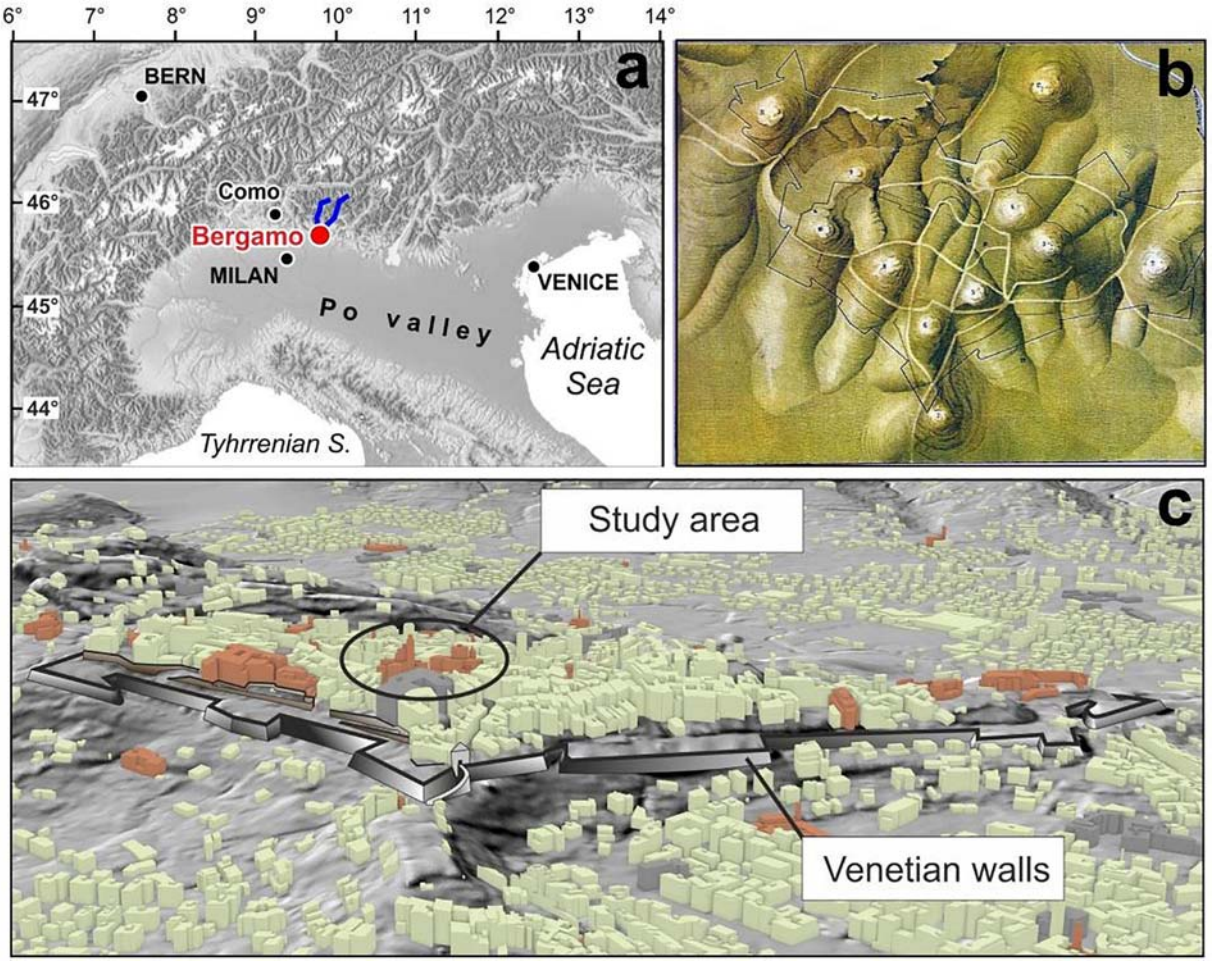

Fig. 1. Geography of the hilltop city of Bergamo. (a) Bergamo at the southern fringe of the Alps. Blue tracks underline the two valleys mouthing in the Po valley close to the Bergamo Hill; (b) paleotopography of part of the Bergamo Hill in an early reconstruction by Fornoni (1890); (c) The modern hilltop town of Bergamo, enclosed by the defense walls built by the Republic of Venice in 1561–1588. View of the old city from the South (GIS elaboration based on Database Topografico del Comune di Bergamo). (For interpretation of the references to color in this figure legend, the reader is referred to the web version of this article.)

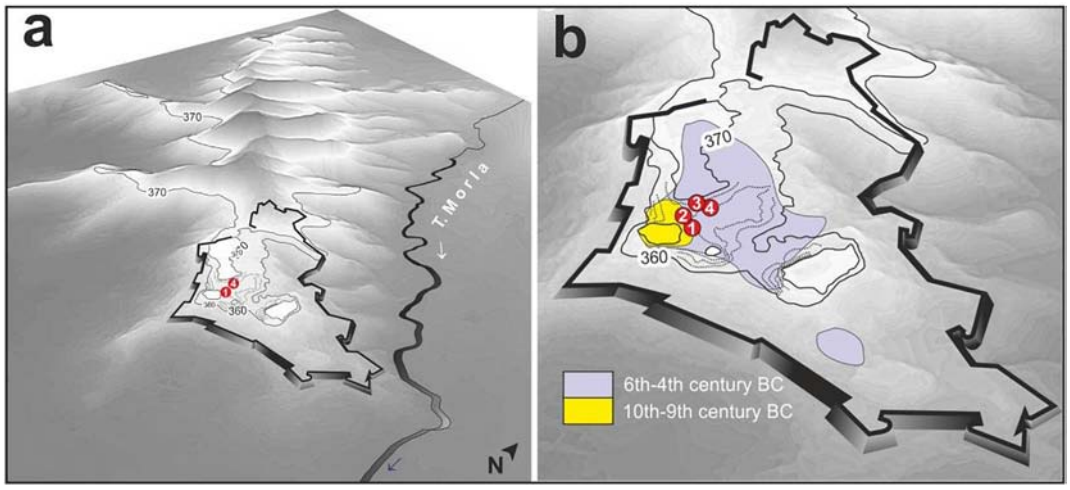

Fig. 2. Topograhy of the ancient settlement of Bergamo. (a) The Hills of Bergamo (*Colli di Bergamo*) and the River Morla in a view from the East, highlighting the Venetian walls (see Fig. 1c) enclosing the hilltop ancient city; main drilling sites 1 and 4 are also shown. (b) Two steps of the development of the ancient settlement (based on Poggiani Keller, 2016) on the Bergamo Hill (*Colle di Bergamo*) and location of the studied sites 1 to 4. See caption Fig. 3 and Suppl. Table S1 for site details. Digital topography elaborated in ArcGIS from the Topographic Database of Regione Lombardia.

century BC this settlement extended over the Bergamo Hill, covering an area of 24 ha (Poggiani Keller, 2001; Fig. 2b). Continuous dwelling is now established since the 6th century BC and the foundation of a Roman town (Poggiani Keller, 2007; Fortunati, 2012). This reconstruction fo the earliest history and foundation of the settlement on the Hilltop of Bergam has been recently challenged by archeological

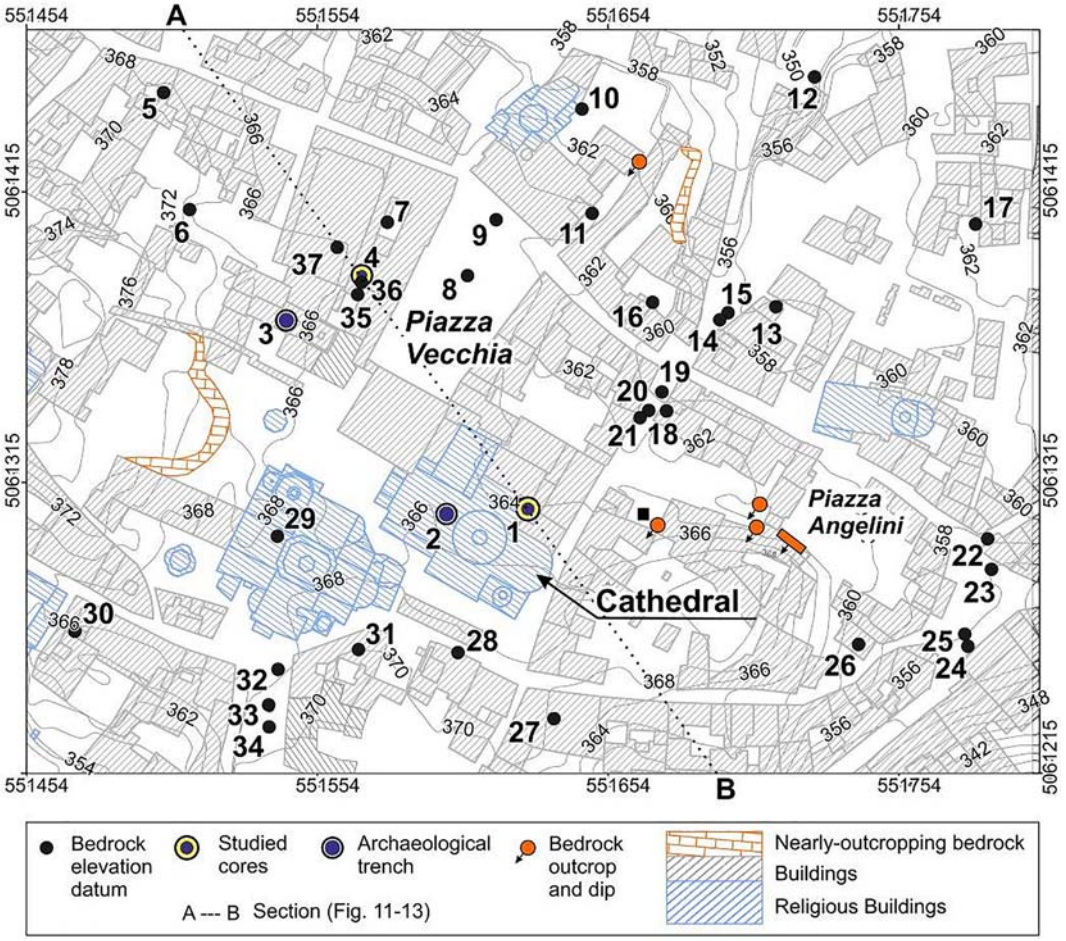

Fig. 3. Subsurface data (drillings and archeological excavations) and field geological survey data used to constrain the paleotopographic bedrock reconstruction. The main sites providing the stratigraphic evidence are numbered 1 to 4. 1 – Cathedral main core, drilled from the modern floor of the Cathedral down to bedrock; 2 – Cathedral trench C, i.e., an archeological trench excavating the Roman and pre-Roman sequence down to bedrock. It underlies the remains of an early Christian church within the Cathedral complex. 3 – *Domus dei Bragagnoli* trench C, i.e., an archeological trench excavated in the basement of the medieval *Palazzo del Podestà* complex. 4 – *Palazzo del Podestà* core S2, drilled from the floor of the medieval complex building, ancient seat of the Podestà. Coordinates are given in WGS84 UTM32. See Suppl. Table S1 for point coordinates and data credits and Suppl. Fig. S1 for a picture of bedrock outcrop.

excavations beneath the Catholic Cathedral (hencefore "Cathedral") and the *Palazzo del Podestà* (Fig. 3), which uncovered ceramics and artifacts dating to early Iron Age phases of the Golasecca culture (Poggiani Keller, 2012, 2016, Fig. 2b). The recognition of an earlier settlement on the Bergamo hilltop, predating the establishment of the urban center, would find comparanda with similar phenomena of cultural continuity documented since the Late Bronze Age in other main centers belonging to the Golasecca culture, located at the Alpine foothills, most notably the city of Como (Fig. 1a, Casini et al., 2001).

Poggiani Keller (2016) proposed that the foundation of the settlement on the Bergamo Hilltop was favored by local resources facilitating agriculture and pastoralism, and the relief providing natural defenses. Furthermore, the strategic position of the hill at the mouth of two of the major Alpine valleys (Fig. 1a), likely attracted regional exchanges both from the Alps (mining and charcoal productions) and from populations inhabiting the Po Plain, notably the Veneti and the northernmost Etruscan groups (Poggiani Keller, 2001).

Thanks to programs of building restoration in the medieval hearth of the ancient city of Bergamo (years 2005–2012), we had access to the sediment record underneath the archeological deposits (*sterile* layer) in the area of *Piazza Vecchia* (Fig. 3). Preliminary radiocarbon dating and paleoecology (Chiesa and Pini, 2008; Pini et al., 2016) inspired the working hypothesis, developed in this paper, that the area around the *Piazza Vecchia* had preserved the environmental record of uninterrupted human activities dating to the Bronze Age, thus predating the earliest archeological evidence at today published.

3. Materials and methods

3.1. Bedrock geology, geoecology and pedoclimate

The Bergamo Hills are shaped in the northern flank of a gentle syncline, inclined southward, deforming stratified rocks of Cretaceous age (Bergamo Flysch, Gelati and Passeri, 1967). These sandstones and pelites are remarkably variable in composition from litarenite to calcarenite, but mostly bear a calcite-cemented silicoclastic fraction (Bersezio et al., 2013). After carbonate leaching, the parent material releases residual quartz, feldspars and clay minerals, which accumulate at the foothills, chiefly into low-order stream valley floors, forming silty-sandy colluvial wedges and paludal alluvial fills of plurimetric thickness. Interestingly, colluvial–alluvial belts and fans occur even on the topmost interfluvial plateaux, and their occurrence in the subsurface of the urban center was already postulated by early scholars (Fig. 1b). The natural soils that evolved in these belts are generally deep and carbonate-free, with high water capacity, udic moisture regime, and low saturation of the exchange complex (Bonalumi et al., 1992; Dystric Cambisols according to WRB, 2015). Leaching, water capacity and runoff are enhanced by a humid regional climate (precipitation 1250 mm/year, Crespi et al., 2018) with significant orographic rainfall in summer, excluding soil drought periods on gentle and north-facing slopes. Low infiltration of low-fractured sandstone and thick colluvial aprons provide water reservoirs especially on north-facing catchments. Paleoclimate studies show that an oceanic climate marked by summer orographic rainfall established in this district of the Italian Alps in the Late Holocene (Holocene global chronostratigraphy according to Walker et al., 2019) as part of the broader reconfiguration of the climatic system taking place 6.5–4 kyrs ago (Furlanetto et al., 2018).

In the present work we adopted the lithostratigraphic and structural assessment provided by the state geological mapping of the Bergamo Flysch (Bersezio et al., 2012, 2013). Interestingly, the studied area is crossed by the so-called "Missaglia Megabed" (Bersezio et al., 2013), a 30 m-thick horizon of limestone, cropping in scarps (Suppl. Mat. 1). This horizon is used in GIS topographic reconstruction (Fig. 4d) to analyze its structural control over the buried bedrock relief and to disentangle possible implications to the environmental setting underlying the growing of the town (Section 6).

3.2. Study area. Subsurface data and spatial reconstruction of bedrock topography

The distribution of archeological finds pre-dating the Celtic urban center (i.e. earlier than the 6th century BCE) on the Bergamo hilltop is limited to a small area South of the *Piazza Vecchia*, which is considered the location of the earliest settlement on the hilltop (Fig. 2b). Here, the Iron Age archeological layers are underlined by thick natural deposits, which were accommodated into mesoscale depressions (Chiesa and Pini, 2008). The potential for paleoenvironmental research prompted investigating the bedrock topography. Lanza (2003) surveyed the elevation of the bedrock surfaces uncovered during archeological excavations. Further data, especially drillings, were made available in the last decade and implemented in an updated database including coordinates (WGS84/UTM32), surface elevation, and bedrock surface elevation (Suppl. Table S1). This layer has been integrated in the Topographic Database of Regione Lombardia (www.http://www.geoportale.regione.lombardia.it/) together with other digital spatial layers such as building blocks and elevation points. Additionally, the elevation of bedrock outcrops (Fig. 3, see Section 3.1.) was used to constrain the interpolation process. The bedrock topography was reconstructed using geostatistical interpolation analysis. We tested several interpolation methods, such as Inverse Distance Weighted (IDW), Radial Basis Functions (RBF) (also known as Spline method) and universal Kriging, the latter was chosen for the final elaboration (Fig. 4), in light of its widespread use in the literature and suitability to the available dataset (Mauel et al., 2013).

3.3. Stratigraphic records, sediment lithofacies, magnetic susceptibility

Two drilled cores and two archeological trenches (Fig. 3) were analyzed for sediment chronostratigraphy and paleoecology.

Cores were obtained by technical rotation drilling, 10 cm-diameter, down to bedrock, operating directly from the floors of the monumental buildings (i.e. site 1 – the Cathedral and site 2 – *Palazzo del Podestà*) by technical rotation drilling working indoor in confined spaces. The lower segment of both cores was heavily consolidated by the static load of the buildings, allowing the core to be effectively longitudinally cut by a steel saw. The resulting surface was polished using a 40 μm smearing sheet and inspected at the stereomicroscope for sedimentary, soft deformation structures, microcharcoal (>200 μm), rock and baked clay fragments identification. Close-up micrographs were taken by an annular flash to avoid reflected light.

Trenches' sections (sites 2 and 3) were inspected and sampled after the completion of archeological excavations down to the "sterile layer," i.e., devoid of cultural materials. Stubbornly, we further deepened the archeological trenches, until reaching deposits underneath the lowermost layer containing macroscopic charcoal. Thus, allowing to date the earliest macroscopic charcoal detectable in the exposed sequence and to sample associated deposits for paleocological analysis (UBA 19904, *Domus dei Bragagnoli* trench C).

Sediment and soil macroscopic components were described on clean surfaces at a 40x stereomicroscope and smear-slides, using reference guides (Jones et al., 1999; WRB, 2015).

Volume magnetic susceptibility (κ 10^{-5} SI) was measured at sites 1,2 and 4 with a Bartington MS2 device equipped with a MS2E core logging sensor (see Dearing, 1999). Measures were taken on dry sediment, before longitudinal cutting, every 2 cm and repeated twice to check environmental conditions changes. The general interpretation of κ values relies on the following assumptions: (a) we take the κ value statistics for the environmental materials (Dearing, 1999; Lees, 1999) as measured into the parent material (bedrock) and its natural weathering products. The materials carrying magnetic properties consists in paramagnetic minerals (e.g. micas) or fire-derived ferrimagnetic components (Oldfield, 1999; Gedye et al., 2000). They occur in the natural colluvial deposits at the base of *Palazzo del Podestà* core, with a κ

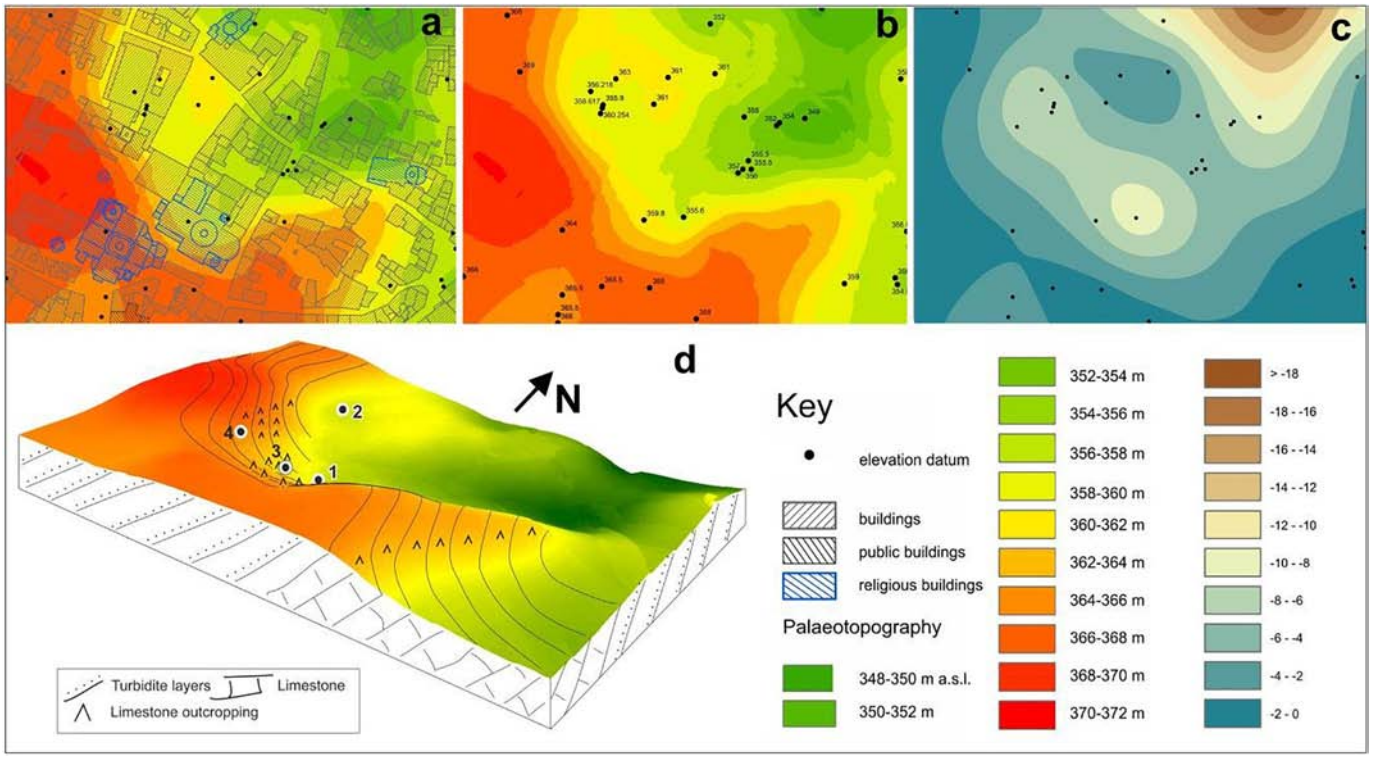

Fig. 4. Reconstructed bedrock topography (a) overlapped by the extant building layer; (b) showing the bedrock elevation data; (c)map of sediment cover thickness; (d) View of bedrock paleotopograhy from SE. The emergence of a limestone bank marks a step-rise in the bedrock relief, suggesting differential erosion of turbiditic sandstone, higher than limestone.

distribution range between 5 and 30 10^{-5} SI (Figs. 7 and 11). In these weathered materials we couldn't identify concentration of magnetite or other ferrimagnetic components, carrying a strong positive susceptibility; (b) we characterized the κ values on individual sediment components in a domestic dump of Early Iron Age, pointing to a link between domestic fires and input of susceptibility-enhancing burnt particles by soil middening, with values $\kappa = 78(\pm 11) \times 10^{-5}$ SI (Suppl. Table S2). (c) Furthermore, we associated the visual identification of artifact sedimentary products, i.e., baked clay particles identified at the 40x-stereomicroscope, with their measured κ values. The occurrence of artifact baked particles invariably resulted in κ peaks exceeding the environmental values, i.e., $\kappa > 50\ 10^{-5}$ SI for scattered ceramics particles in the size of fine sands, while reaching up to 220 10^{-5} SI for individual brick fragments of centimetric size. All these measurements agree with reference magnetic enhancements of (b) burnt soils and (c) baked clay from archeological sites with respect to (a) environmental materials (Jordanova et al., 2001). An upper threshold value of $\kappa = 30\ 10^{-5}$ SI, roughly indicating the maximum κ value locally measured in environmental materials, is shown in Figs. 7 and 11.

3.4. Radiocarbon dating and archeological chronology

From the four sedimentary sequences (sites 1–4) we radiocarbon-dated charred wood and caryopsis, avoiding any bulk sample. To prevent contamination while processing samples, macroscopic charcoal fragments and fruits were visually inspected and picked under the stereomicroscope, taxonomically identified, dried out, and weighed promptly, ensuring at least 0.01 g of dry organic matter for each sample. We excluded presence of old wood effect from individual stratigraphic layers either by measuring a sample of caryopsis and one of charred wood (samples Ub 40937/Ub 40939 Cathedral trench C) or by stratigraphically cross-validating the obtained results in a laminated, continuous sequence (samples Ub 40941/Ub 42140/Ub 42141/Ub 42142, Cathedral main core). The statistical identity of ages provided by the same level was χ^2 tested and eventually pooled. AMS-radiocarbon ages were calibrated using Calib 7.0.2 (Stuiver et al., 2013) and Oxcal v4.3 (Bronk Ramsey, 2017; Bronk Ramsey and Lee, 2013) based on the IntCal 13 calibration curve (Reimer et al., 2013). The chronological model was built using OxCal v4.3. Due to important changes in sedimentary rates along the sedimentary sequences, we adopted a low flexibility model ($K = 0.01$). See Suppl. 3 for OxCal CQL2 code. In Fig. 10 and Suppl. Fig. S2, the posterior density estimates output by the model are shown in black, with the unconstrained calibrated radiocarbon dates shown in outline. See Suppl. Table 4 for the complete posterior Bayesian statistics.

Radiocarbon calibrated ages are presented both in yrs. cal BP and in yrs. cal BC/AD in order to compare them with the archeological chronology. The latter is given in centuries BC/AD followed by the respective authority publishing the supporting pottery typology. Archeological periodization follows De Marinis (2014). To avoid confusion, we avoided reporting calibrated probability intervals in the text; instead we used only the median probability of calibrated ages. When reporting modeled sequences (a posteriori density estimates), we used modeled calibrated median probability and $2\sigma +/-$ ranges modeled calibrated distributions.

3.5. Geopedochemistry

Concentrations of phosphorus forms (total, organic, inorganic and available P) were determined on sediments from the Cathedral main core following soil chemistry procedures (Colombo and Miano, 2015). Total P was extracted by hot aqua regia treatment in microwave oven after organic matter removal with hydrogen peroxide. Organic P was calculated as difference between P obtained after sulfuric acid treatment with and without heating at 550 °C; inorganic P was obtained as difference between total and organic P. Available P was extracted with sodium bicarbonate (Olsen method). After extraction, the P forms were

determined spectrophotometrically via blue phosphomolybdate complex.

Samples for C/N determination were analyzed by dry oxidation after carbonate removal by HCl, to determine soil organic carbon and total nitrogen content (Flash EA 1112 NCSoil, Thermo Fisher Scientific elemental analyzer, Pittsburgh, PA, USA). Total K was extracted in aqua regia in microwave oven and determined through AAS (atomic absorption spectroscopy).

3.6. Paleoecology and archeobotany

Pollen, spores, microscopic charcoal fragments and other biological particles were extracted from 90 sediment samples obtained from the Cathedral and *Palazzo del Podestà* cores and from *Domus dei Bragagnoli* trench C (see Figs. 5, 7, 8b for sampling stratigraphy). Preparation of samples followed standard methods at the Lab. of Palynology and Palaeoecology of Milano, including HF and acetolysis. *Lycopodium* tablets were added for pollen and charcoal concentration estimation (Stockmarr, 1971). Pollen identification relies on Punt and Blackmore (1976-2009), Reille (1992-1998), Beug (2004) and the CNR-IGAG reference collection. Pollen zonation was obtained by a constrained incremental sum of squares cluster analysis, using the Cavalli Sforza's chord distance as dissimilarity coefficient (CONISS, Grimm, 2015). Pollen % plotted in Figs. 10–11 refer to the sum of trees, shrubs and upland herbs. Quantitative paleoecological proxies were obtained from cumulating percentage values of recognized diagnostic pollen, spore and

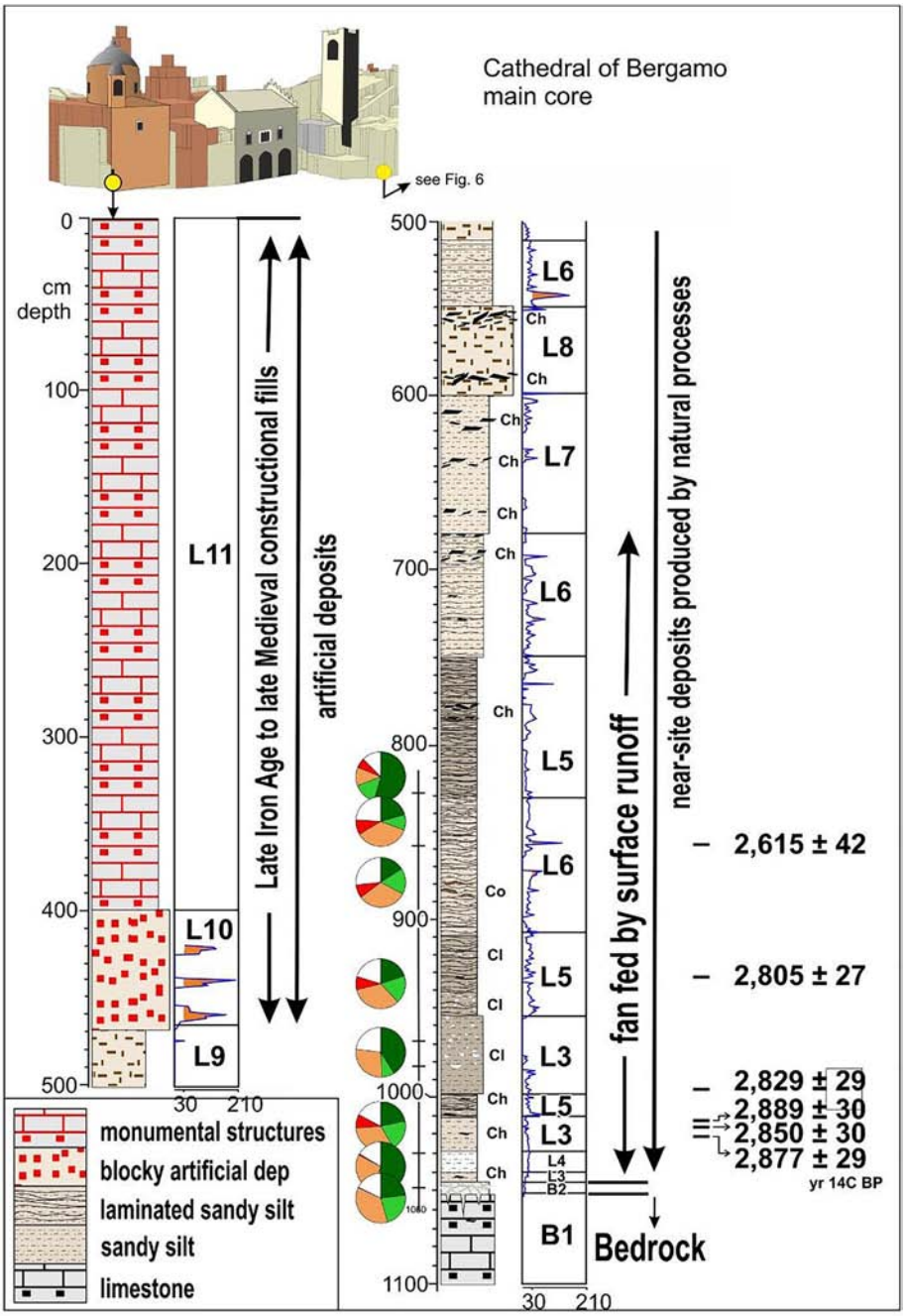

Fig. 5. Site 1 – Cathedral main core, in the ancient city of Bergamo. Lithostratigraphy, magnetic susceptibility, summary pollen data (pie charts, each one averaging a pollen zone; keys to pollen pie charts in Fig. 7) and uncalibrated radiocarbon dating. L = Lithofacies, B = Bedrock (see Fig. 6). Ch = Macrocharcoal accumulations. Cl = Rock fragments, size >0.5 mm. The interval 550–600 cm depth was not measured for magnetic susceptibility.

parasite types (see Table 1). Two size classes of pollen-slide charcoal particles were counted (10–50 and 50–250 μm length). This paper presents paleoecological proxies of land use and nutrients, while the complete biodiversity will be fully described and explored in a separate paper (Pini et al., in prep.). All the studied material is stored at the CNR repository currently hosted at CNR-ARM3, Milano.

The analysis of macroscopic plant remains (fruits and seeds but also other plant debris) from Cathedral trench C was carried out on five samples (average volume of 1.35 l; see stratigraphic position in Fig. 7), whereas three samples (average volume of 1.86 l) were analyzed from *Domus dei Bragagnoli* trench C for the time period Bronze Age/Early Iron Age. The samples were wet sieved at 1 and 0.35 mm mesh sizes using the wash-over method (Hosch and Zibulski, 2003). The samples were sorted using a Leica/Wild M3C stereomicroscope with a 6.4–40x-magnification. Identifications were made using the CNR-IGAG reference collections, in addition to the specific literature (Cappers et al., 2006; Neef et al., 2012; Jacomet, 2006).

Macroscopic wood charcoal was analyzed from a total of eight sediment samples (average volume ca. 2.29 l) collected from the *Domus dei Bragagnoli* trench C, dating to the time period here discussed (Bronze Age–Early Iron Age). Charcoal fragments were extracted through wash-over method (Hosch and Zibulski, 2003). The fragments larger than 2 mm were observed in the three main sections (transverse, tangential, radial) under an episcopic microscope (Zeiss Axio Scope A.1) equipped with dark field/bright field illumination system. Botanical identification is based on comparison with wood atlases (e.g., Schweingruber, 1990a, 1990b; Jacquiot et al., 1973) and the CNR-IGAG modern reference collection.

In the present paper the macrofossils will be used to constrain the environmental inferences.

3.7. Development of a multidisciplinary environmental reconstruction

The bedrock topography helped envisaging land-use units based on suitability to plowing (i.e., gentle slopes) and to animal husbandry (steeper slopes). A first land-use surface classification was then matched with information collected at studied sites 1–4 and with archeological excavations, providing a preliminary spatial layer of settlements, middens, ruderal and dumping areas in the 9th century BC (Poggiani Keller, 2016, see Fig. 2). Hence, we proceeded to reconstruct the time window of 2850–2750 yrs. cal BP, i.e., the 9th century BC (onset of the Iron Age) supported both by on-site data, and by data on sedimentary processes and/or quantitative paleoecology at the studied near-site cores and trenches. We afforded depositional issues dealing with pollen and spore proxies in terrestrial environments (i.e., airborne versus runoff-floated, and selective deterioration processes) examining their relationships with natural and anthropogenic sedimentary processes (e.g., Edwards, 1991; Ravazzi et al., 2019) and relevant pollen source area in mountain regions (Marquer et al., 2020).

4. Results and interpretation

4.1. Bedrock topography

The studied area is located on the NE slope of the hilltop area, a location expected to be deeply entrenched by slope valleys according to early studies about the Bergamo Hill morphology (Fornoni, 1890; Fig. 1b). The GIS-reconstructed bedrock topography confirms a valley track emerging on the NE side of the studied area (Fig. 4), but also points to a sharp step-rise oriented NW-SE, scaling a hilly summit at an elevation of 364–368 m a.s.l. from a depressed flat surface at 355–363 m a.s.l. The flat area records a significant thickness of sediment cover, reaching over 10 m in the footslope belt, forming a platform running beyond the monumental buildings of the Cathedral and the *Palazzo del Podestà* (Fig. 4c). Both the studied cores are placed at the footslope of the bedrock step-rise. Drilling number 1 (Cathedral main core) approaches the headwall of the valley emerging on the NE side, this is situated at first Strahler's stream order. The bedrock step-rise at the valley headwall is likely controlled by the geological structure, i.e., the emergence of a limestone bank, dipping SW (Section 3.1. and Suppl. Fig. S1). These landforms do not leave any trace in the modern topography, hidden by the thick sediment platform on top of which the modern city is built.

4.2. Sediment stratigraphy

The stratigraphic interpretation of the sediment infill is primarily based on cores drilled below the modern Cathedral (site 1 – Figs. 5 and 6) and the *Palazzo del Podestà* (site 4 – Figs. 6 and 7). Results are graphically summarized in Fig. 6. In this work we are considering exclusively the natural deposits forming the lowermost core segments dating to the Bronze Age and on the sedimentary processes recorded in nearby archeological deposits (sites 2 and 3).

4.2.1. Cathedral main core

The sediment cover resting on limestone bedrock is formed by a thin regolith layer (Fig. 6b) immediately overlain by massive, well-sorted carbonate-rich silt chaotically imbedding scattered macrocharcoal particles and rock fragments of micritic limestone (L3 – Fig. 6a). The lowermost dated macrocharcoal fragment was observed just 5 cm above the

Table 1
Pollen, spores and parasite types grouping adopted for quantitative ecological proxies of vegetation and land-use.

Groups represented in pie charts and histograms, Figs. 5-6-10-11	Color used for group representation	Diagnostic pollen, spore or parasite types	Proxies for
Trees	Green	Sum of arboreal pollen (AP): *Carpinus betulus*, deciduous *Quercus, Alnus glutinosa* type, *Betula* and *Fagus*	Forests
Shrubs	Light green	Sum of *Calluna, Corylus, Hedera, Polygala, Rubus, Salix, Sambucus nigra* type	
Anthropogenic habitats	Red	Cereals (see below), *Linum usitatissimun, Vitis, Vicia* type, *Orlaya grandiflora*, Scrophulariaceae, *Sanguisorba minor, Helianthemum, Centaurea scabiosa–nigra–cyanus* type, *Asphodelus, Plantago media* type and *P. lanceolata, Trifolium* type, *Convolvulus, Verbena, Malva, Euphorbia, Polygonum aviculare* type	Cultivated plants, pastures, dry fallows
Coprophilous spores and intestinal parasites	Black	*Sordaria, Apiosordaria, Sporormiella, Cercophora, Podospora, Arnium, Delitschia, Tricodelitschia, Trichuris*	Presence of livestock, grazing habitats
Pastures	Black	*Orlaya grandiflora*, Scrophulariaceae, *Sanguisorba minor, Helianthemum, Centaurea scabiosa–nigra–cyanus* type, *Asphodelus, Plantago media* type and *P. lanceolata, Trifolium type*	Dry fallow, dry to drained pastures
Cereals	Black	Sum of Gramineae with grain diameter > 47 μm and annulus >11 μm (group including almost all species of the genus *Triticum*, *Hordeum* and *Avena sativa*) and Gramineae >47 μm < 11 μm (group mostly formed by cereals and including *Secale*, and some cereal weed like *Avena* and wild *Bromus* species)	Cereal fields
Gramineae	Orange	Sum of Gramineae pollen, regardless of grain size	Natural grasslands and cereal fields
Other terrestrial herbs	White	Sum of terrestrial herbs not included in other groups	Herb communities

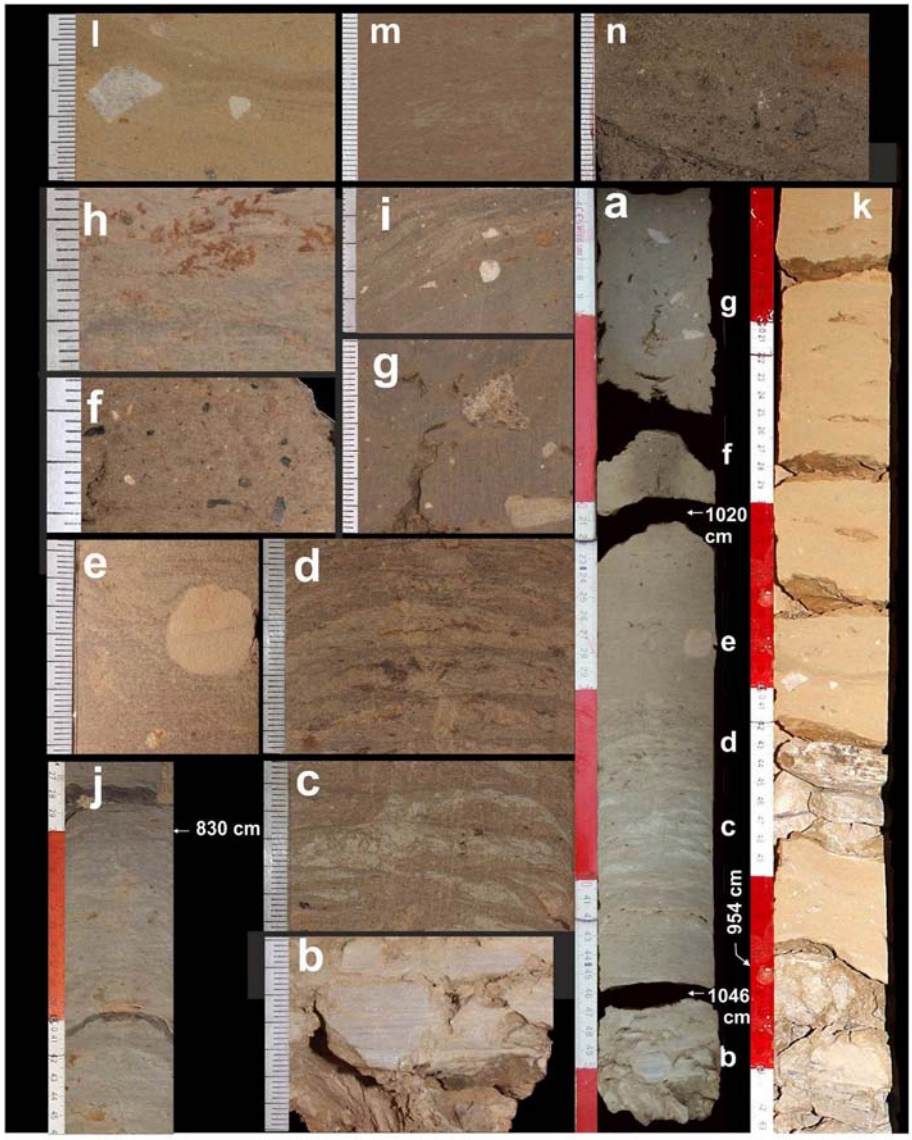

Fig. 6. Sites 1 and 4. Lithofacies, sedimentary and soft-deformation structures. Panels a–j from the Cathedral main core. Core hemicylinders (a, j) and details of lithofacies (b–i). Panel lettering according to stratigraphy, from base to top: (a) core segments 1053 to 1002 cm depth; (b) Detail of regolith formed by micritic limestone clasts with brown silty clay matrix, resting on bedrock (B2-1053–1045 cm depth); (c) Lenticular-stretched structures produced by coring operations deforming light carbonate-rich and hydroxides-rich silty laminations (1039–1036 cm depth); (d) Lenticular-stretched structures deforming carbonate-rich and hydroxides-rich laminations (L4-1035–1031 cm depth); (e) A rounded weathered limestone lithorelict fragments imbedded in carbonate silty sand matrix rich in Fe–Mn hydroxides (1030–1026 cm depth); (f) Massive carbonate-rich silt rich in macrocharcoal particles and imbedding rock fragments of micritic calcite (L3-1017–1015 cm depth); (g) Laminations formed in a carbonate silty matrix, deformed by coring operations, imbedding calcarenite fragments and a framestone rock fragments (1012–1008 cm depth); (h) Alternances of poached laminations of carbonate-rich silt (dark) and sand (yellow), the voids precipitated by Fe-hydroxides (L5-927–924 cm depth); (i) Millimetric and submillimetric alternances of laminated carbonate-rich silt and sand, deformed by coring operations, imbedding micritic limestone and hydroxide nodules (L5-918–913 cm depth); (j) Laminated sediment alternances showing liquefied sand veins and lenticular structures. Darkening upwards marks an increase of organic matter paralleled by changes in organic biochemistry (see Section 5 and Fig. 11). (L6-846–827 cm depth). Panels k–n from *Palazzo del Podestà* core S2. Core hemicylinder (k) showing weathered, massive silty sands overlying the contact to regolith (958–954 cm depth) and bedrock (>958 cm depth); (l) massive, well-sorted fine sands; (n) lenticular sequence of sands with microcharcoal accumulations. (For interpretation of the references to color in this figure legend, the reader is referred to the web version of this article.)

regolith (modeled age 2984 + 70/−37 yrs. cal BP, i.e., 1034 + 70/−37 yrs. cal BC, see Section 4.3). These deposits provided palecological evidence of extensive farming (Section 5). Good preservation of organic microfossils suggests sediment water saturation or waterlogging. This sequence onset is formed by massive slope deposit admixing both regosols and anthropogenic soils components but lacking baked clay and other artifacts. Those massive deposits are followed by a 280 cm thick, millimetric and submillimetric alternance of silt-chips in laminated, often sharply interrupted and/or casted by soft deformation, poorly sorted carbonate-rich silt and fine sand, imbedding micritic limestone and hydroxide coatings relicts (L5–L6, details in Fig. c–d–f–g–h–i). Imbedded are massive sands with rock fragments and pedorelicts (Fig. 6e). Deformation by coring operations produced horizontal stretching and faulting of sedimentary structures (Fig. 6c). Because of widespread undulations in lamination, deposition was likely driven by sheet flows decanted into shallow water. Poor selection and lack of tractive structures would exclude significant alluvial processes. This type-sequence, also including mud flows, is observed in the development of waterlogged colluvial fans and aprons at the footslope (Schoeneberger et al., 1998; Strahler and Strahler, 2007). The whole sequence contains massively transported wood macrocharcoal (Fig. 6f), but no distinct charcoal accumulations beds. Excellent preservation of palynomorphs

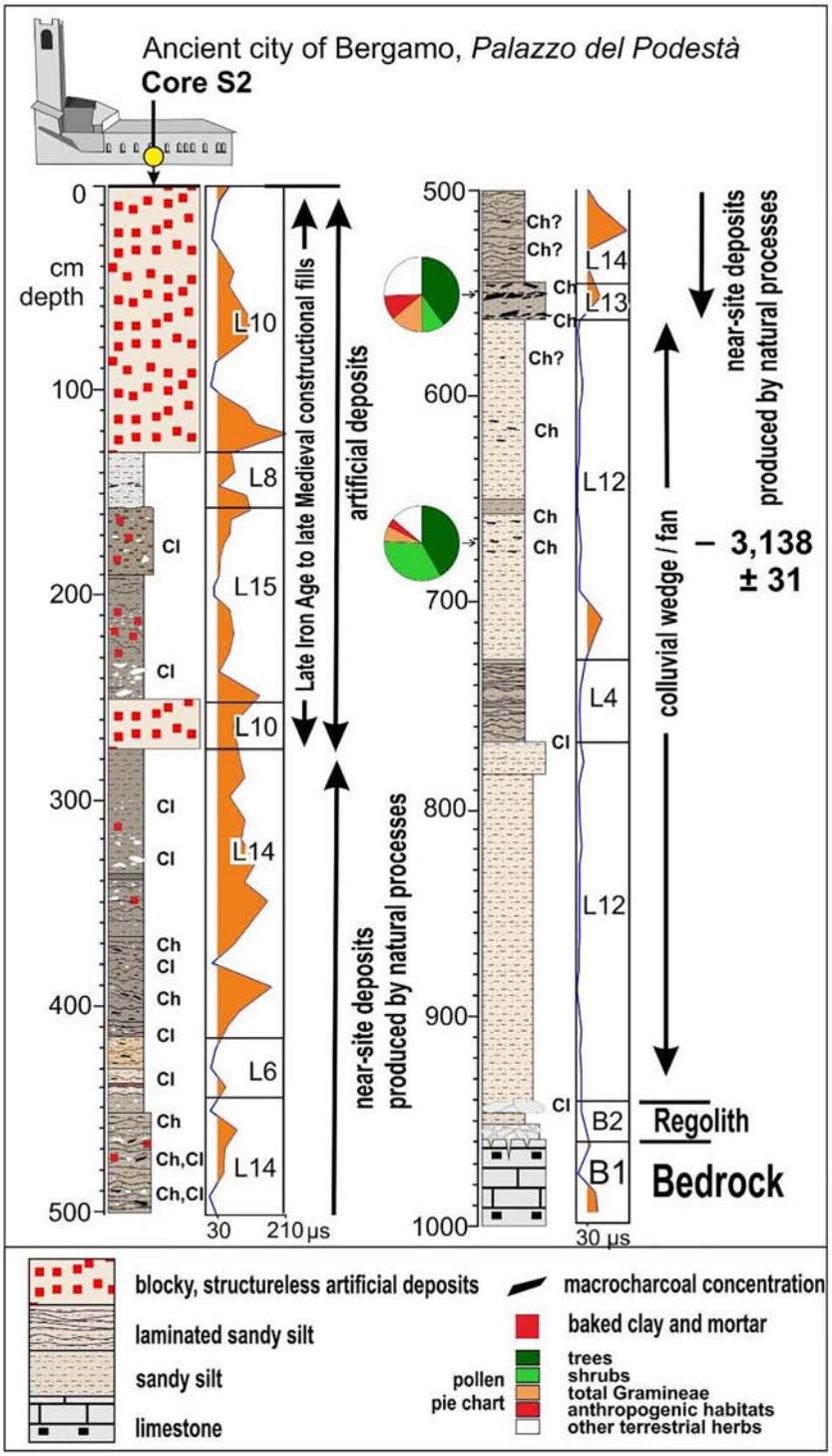

Fig. 7. Site 4 – *Palazzo del Podestà* core S2. Lithostratigraphy, magnetic suceptibility and uncalibrated radiocarbon dating. Ch = Macrocharcoal accumulations; Cl = Rock fragments, size >0.5 mm; L = Lithofacies; B = Bedrock.

indicates a water-saturated sediment or waterlogging. Furthermore, persistent lamination, widespread crumpling of laminae in chaotical patterns (Fig. 6h), high phosphorus concentration (Section 5) and the very low stream order predicted by paleotopographic setting (Section 4.1) suggest sedimentation in a pond with bioturbation. Animal poaching and herb root casts may explain the observed sediment features (Laporte and Behrensmeyer, 1980; Rentzel et al., 2017; Wilson and Everard, 2017). We therefore argue that the drilling intercepted the infill sequence of a pond used for livestock watering. Such a circumstance is also supported by paleoecological data, suggesting intensive farming and pastoralism in the pollen source area (Section 5). According to the sequence ages, deposition occurred quite rapidly. Darkening upward marks the laminated sequence starting at level 830 cm depth onward (Fig. 6j and Section 6). The whole sequence up to 600 cm depth lacks any fragment of baked clay, a circumstance which is also excluded by the volume susceptibility κ values which remain below 30×10^{-5} SI (Fig. 5). The overall sedimentological picture points to a deposition which is near-site to a human settlement, but

well out of the limits of middens, ruderal and dumping areas (near-site type B in Ravazzi et al., 2019). Intensive runoff at the waterlogged foot of steep slopes occupied by pasture and arable fields may indeed explain the observed sedimentary pattern. Constructional deposits of Roman and Medieval age form the uppermost 470 cm of the sequence (L10).

4.2.2. Palazzo del Podestà core S2

The calcarenite bedrock is covered by a thin regolith layer, followed by a 370 cm-thick unit of massive, well-sorted fine sands rich in carbonate and micas (L12), often imbedding micaceous calcarenite rock fragments (Fig. 6l). This unit may represent a massive colluvial apron, with only a laminated interval (L4) recalling sheet flows. Macrocharcoal particles >0.5 mm and artifacts are absent in the basal 300 cm sediments. First scattered macrocharcoal fragments occur in these fine sands since 671 cm depth onward. A sharp, erosional boundary separates these natural deposits from a distinctive micaceous sand imbedding several accumulations of lenticular microcharcoal (L13) at 565–547 cm depth (Fig. 6n). Given the lenticular charcoal accumulation, peaks of magnetic susceptibility (κ values $>50 \times 10^{-5}$ SI, Fig. 7), and microbotanical evidence of intensive farming (Section 5), this layer is interpreted as a midden, in a near-site position (near-site type A in Ravazzi et al., 2019). It is followed by an anthropogenic soil (L14), formed by lenticular silty sands, rich in macrocharcoal and baked clay fragments, and still recording high values of magnetic susceptibility. The uppermost 275 cm are made by constructional deposits of Roman and Medieval ages (L10/L15).

4.2.3. The archeological trenches providing evidence of human activity in the Bronze Age and Early Iron Age

The Cathedral trench C (site 2) exposed dumping layers dated to the Early Iron Age (see Section 4.3), gently sloping NE, in agreement with the reconstructed paleotopography (SU 1022–SU 420b in Fig. 8a). Each layer represents a close sequence of connected events of either human-acted dumping of coarse slope deposits, including ceramic fragments (SU 429), and dark-brown silt, rich in amorphous humified organo-mineral, microcharcoal and fire-derived ferrimagnetic components (see Suppl. Table S2) typical for domestic dumps and topsoils in ruderal areas. The charred seed and fruit assemblages sieved out from dark silty layers speaks for crop fields and wet fallow land, ruderal and wetland habitats (Fig. 8a). The Early Iron Age sequence is truncated by Roman constructional structures (Ghiroldi, 2019). The *Domus dei Bragagnoli* trench C (site 3) exposed a complex sequence of 360 cm

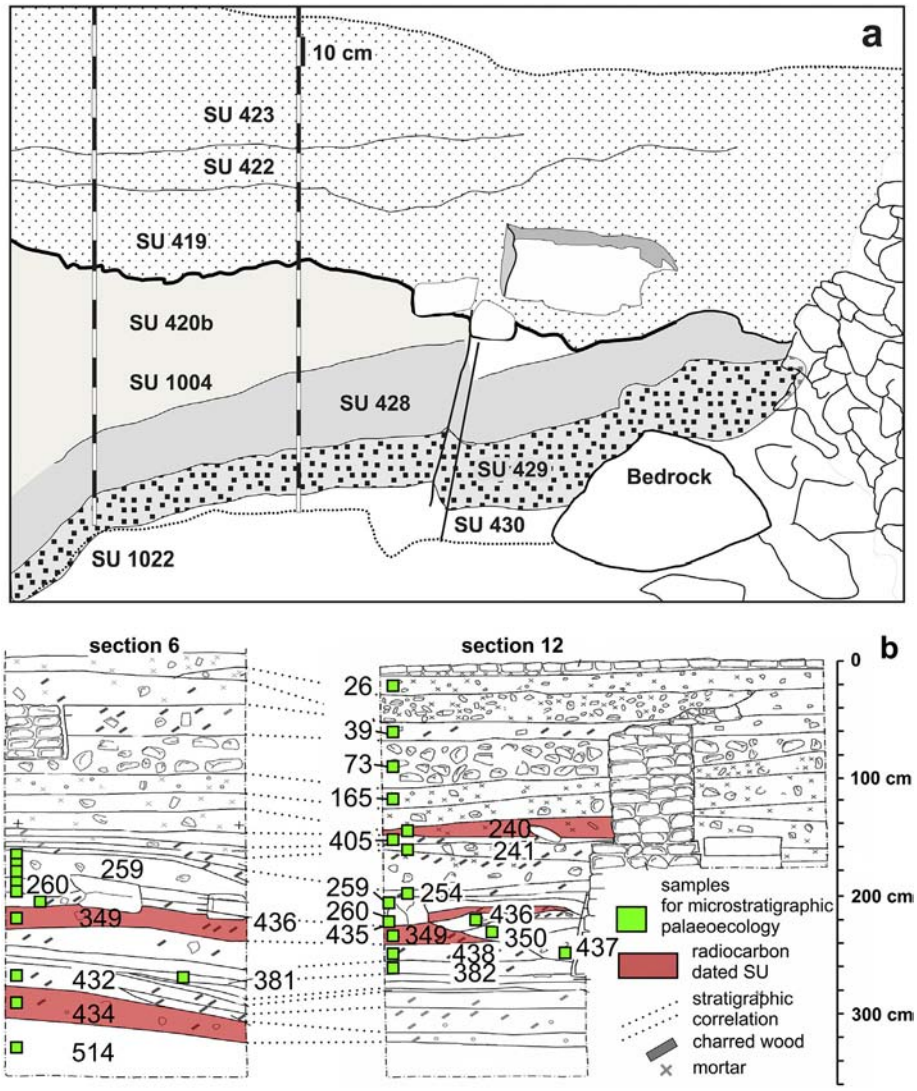

Fig. 8. a) Site 2 – Cathedral trench C, profile drawn during sampling, stratigraphic interpretation (outlined). Black and white bars on the meter are 10 cm long; b) Site 3 – *Domus dei Bragagnoli* trench C, stratigraphy and microstratigraphic sampling (modified from Pini et al., 2016). (For interpretation of the references to color in this figure legend, the reader is referred to the web version of this article.)

thick near-site deposits spanning from the Late Bronze Age to the Roman and Medieval building activities (Poggiani Keller, 2012; Fortunati, 2012; Pini et al., 2016; Fig. 8b).

4.3. Radiocarbon chronology

A total of 16 radiocarbon measurements are so far available from the four investigated sites, below or around the Cathedral on the hilltop of Bergamo (Table 2). The obtained radiocarbon ages span from the 3450 yrs. cal BP (15th century cal BC) to the Roman period but concentrate in the millennium between 3450 and 2500 yrs. cal BP, the chronological focus of this paper (Fig. 10). The uppermost stratigraphic record, spanning the urban development of the Bergamo town (since the 6th–5th century BC until the Modern Age) was not investigated. Repeated measurements from the same layers provided statistically indistinguishable ages, thus suggesting that old wood effect is not significant in these materials. Single ages from SU 434 and SU 1000 fall in the radiocarbon plateaux at 3450–3200 and 2640–2350 yrs. cal BP (Suppl. Mat. 6) and should be handled with the due cautious. In the interval 3050–2700 cal BP, ages are more robust as calibration ranges are smaller ($\sigma = 12/36$ between 2700 and 2800 yrs. cal BP; $\sigma = 32/44$ between 2750 and 3050 yrs. cal BP).

The oldest age so far obtained from deep layers in the *Palazzo del Podestà* core S2 (Fig. 7) was calibrated to 3359 yrs. cal BP (= 1409 yrs. cal BC, median probability) and modeled 3355 ± 96 yrs. cal BP (1405 yrs. cal BC, Table 2 and Suppl. Table S4). It refers to colluvial deposits bearing paleoecological evidence of human activity (Section 5), devoid of macroscopic artifacts.

At *Domus dei Bragagnoli* trench C (Fig. 8b), basal layers span the interval between 3250 and 3000 yrs. cal BP (1300–1050 yrs. cal BC) and are characterized by a low average accumulation rate. These deposits were found to be devoid of artifacts. The subsequent Iron Age

Table 2
Radiocarbon chronology obtained from the dated stratigraphic sequences.

Lab code	Dated material	Sample weight (g)	Sample provenance (site, depth, US)	14C age (yrs uncal BP)	Calibrated ages (cal yrs BP), 2 sigma interval	Median probabilites (cal BP)	Calibrated ages (cal yrs BC), 2 sigma interval	Median probabilites (cal BC/AD)
Ub 40938	12 grains *Panicum/Setaria*, 1 spikelet fork *Triticum*, 4 glume base, 1 *Triticum* grain	0.0111	Cathedral trench C, SU 431 top	2580 ± 24	2625–2625 cal BP (0,1%) 2710–2757 cal BP (99,9%)	2739 yrs cal BP	808–761 cal BC (99,9%) 676–676 cal BC (0,1%)	789 yrs cal BC
Ub 40937	*Vicia* cf. *faba* seed	0.021	Cathedral trench C, SU 1022	2674 ± 27	2749–2809 cal BP (84,4%) 2814–2844 cal BP (15,6%)	2775 yrs cal BP	895–865 cal BC (15,6%) 860–800 cal BC (84,4%)	825 yrs cal BC
Ub 40939	Charcoal fragment of *Carpinus*	0.3188	Cathedral trench C, SU 1022	2705 ± 25	2759–2851 cal BP (100%)	2802 yrs cal BP	902–810 cal BC (100%)	852 yrs cal BC
Ub 40,943	Charcoal fragments	0.0278	Cathedral main core, 854–856 cm	2615 ± 42	2541–2561 cal BP (1,9%) 2579–2581 cal BP (0,2%) 2618–2631 cal BP (1,5%) 2701–2845 cal BP (96,4%)	2750 yrs cal BP	896–752 cal BC (96,4%) 682–669 cal BC (1,5%) 632–630 cal BC (0,2%) 612–592 cal BC (1,9%)	800 yrs cal BC
UBA 9262	Wood fragment		Cathedral main core, 932 cm	2805 ± 27	2845–2979 cal BP (99,6%) 2986–2991 cal BP (0,4%)	2907 yrs cal BP	1042–1037 cal BC (0,4%) 1030–896 cal BC (99,6%)	957 yrs cal BC
Ub 40,941	Charcoal fragments	0.0118	Cathedral main core, 994–996 cm	2829 ± 29	2854–3006 cal BP (99,1%) 3014–3022 cal BP (0,7%) 3029–3030 cal BP (0,2%)	2931 yrs cal BP	1081–1080 cal BC (0,2%) 1073–1065 cal BC (0,7%) 1057–905 cal BC (99,1%)	981 yrs cal BC
Ub 42,140	Charcoal fragments	0.0059	Cathedral main core, 1012–1014 cm	2889 ± 30	2927–3081 cal BP (90,7%) 3092–3143 cal BP (9,3%)	3020 yrs cal BP	1194–1143 cal BC (9,3%) 1132–978 cal BC (90,7%)	1070 yrs cal BC
Ub 42,141	Charcoal fragments	0.0098	Cathedral main core, 1016–1018 cm	2850 ± 30	2876–3059 cal BP (100%)	2961 yrs cal BP	1110–927 cal BC (100%)	1011 yrs cal BC
Ub 42,142	Charcoal fragments	0.0056	Cathedral main core 1020–1022 cm	2877 ± 29	2887–2908 cal BP (3%) 2921–3077 cal BP (94,5%) 3095–3106 cal BP (1,3%) 3128–3138 cal BP (1,2%)	3001 yrs cal BP	1189–1179 cal BC (1,2%) 1157–1146 cal BC (1,3%) 1128–972 cal BC (94,5%) 959–938 cal BC (3%)	1051 yrs cal BC
Ub 40,940	Charcoal fragments	0.0085	Palazzo del Podestà, core S2, 671 cm	3138 ± 31	3253–3296 cal BP (18,6%) 3324–3414 cal BP (73,4%) 3418–3445 cal BP (7,9%)	3365 yrs cal BP	1496–1469 cal BC (7,9%) 1465–1375 cal BC (73,5%) 1347–1304 cal BC (18,6%)	1415 yrs cal BC
UBA 19900	Charcoal fragments	0.072	Domus dei Bragagnoli, trench C, room 14, sect. S, SU 240	1952 ± 30	1826–1853 cal BP (8,9%) 1858–1951 cal BP (85,9%) 1959–1972 cal BP (3,6%) 1978–1985 cal BP (1,6%)	1903 yrs cal BP	36–29 cal BC (1,6%) 23–10 cal BC (3,6%) 2 cal BC - 92 cal AD (85,9%) 97–124 cal AD (8,9%)	48 yrs cal AD
UBA 19901	Charcoal fragments	0.1	Domus dei Bragagnoli, trench C, room 14, sect. S, SU 435	2942 ± 34	2985–3183 cal BP (97,7%) 3192–3208 cal BP (2,3%)	3099 yrs cal BP	1259–1243 cal BC (2,3%) 1234–1036 cal BC (97,7%)	1149 yrs cal BC
UBA 19902	Charcoal fragments	0.122	Domus dei Bragagnoli, trench C, room 14, sect. S, SU 349	2885 ± 47	2880–2913 cal BP (6,1%) 2917–3159 cal BP (93,9%)	3017 yrs cal BP	1210–968 cal BC (93,9%) 964–931 cal BC (6,1%)	1067 yrs cal BC
UBA 19903	Charcoal fragments	0.03	Domus dei Bragagnoli, trench C, room 14, sect. E, SU 349 (117 cm)	2908 ± 29	2960–3083 cal BP (77,1%) 3090–3156 cal BP (22,9%)	3044 yrs cal BP	1207–1141 cal BC (22,9%) 1134–1011 cal BC (77,1%)	1094 yrs cal BC
UBA 19904	Charcoal fragments	0.032	Domus dei Bragagnoli, trench C, room 14, sect. E, SU 434 (185–188 cm)	3032 ± 29	3157–3279 cal BP (70,8%) 3280–3345 cal BP (29,2%)	3233 yrs cal BP	1396–1331 cal BC (29,2%) 1330–1208 cal BC (70,8%)	1283 yrs cal BC

settlement layers were not submitted to radiocarbon dating, with chronology based on typological dating of the archeological materials therein found.

The lowermost segment of the Cathedral main core (Fig. 5) is soundly dated to 2980–2700 yrs. cal BP (i.e., starting in the 11th century BC, Fig. 9). Here, more than 150 cm of sediment was deposited between 2984 + 70/−37 yrs. cal BP (i.e., 1030 + 70/−37 yrs. cal BC, Ub 42,142, median probability and 2σ range of modeled age; median unmodelled 1050 yrs. cal BC) and 2850 yrs. cal BP, while sedimentation rate remained high and laminated at least until 2753 yrs. cal BP (i.e., 803 + 99/−139 yrs. cal BC, Ub 40943, median of modeled calibrated age and 2σ range median probability). The modeled age for level 830 cm is 2700 yrs. cal BP (2745–2630 2σ range). As shown by sedimentology, this sequence accumulated by the persistent runoff activity in a depressed position connected to farmed slopes.

The dump exposed by the Cathedral trench C (Fig. 8a) formed between 2780 yrs. cal BP (i.e. 830 yrs. cal BC, median probability of the pooled mean ages Ub 40937 and Ub 40939, both obtained from SU 1022) and an undefined time around 2710–2430 yrs. cal BP (i.e. 760–-480 yrs. cal BC, Ub 40936). The wide calibration uncertainty of this age is due to a well-known radiocarbon plateau (Suppl. Fig. S2; Jacobsson et al., 2018).

The match between radiocarbon and paleoecological evidence will be discussed in Section 5.

5. Paleoecological records and chronology of land-use changes

5.1. Microbotanical record

Palynomorphs were recorded from Cathedral main core (site 1), *Palazzo del Podestà* core S2 (site 4) and *Domus dei Bragagnoli* trench C (site 3). Pollen concentrations are high enough to allow for effective counting at the microscope, with sums usually higher than 500 grains of terrestrial plants. Pollen preservation is overall good with corrosion (sensu Cushing, 1967) not preventing identifications. Strong selective pollen deterioration has been observed in two layers of leached sediment

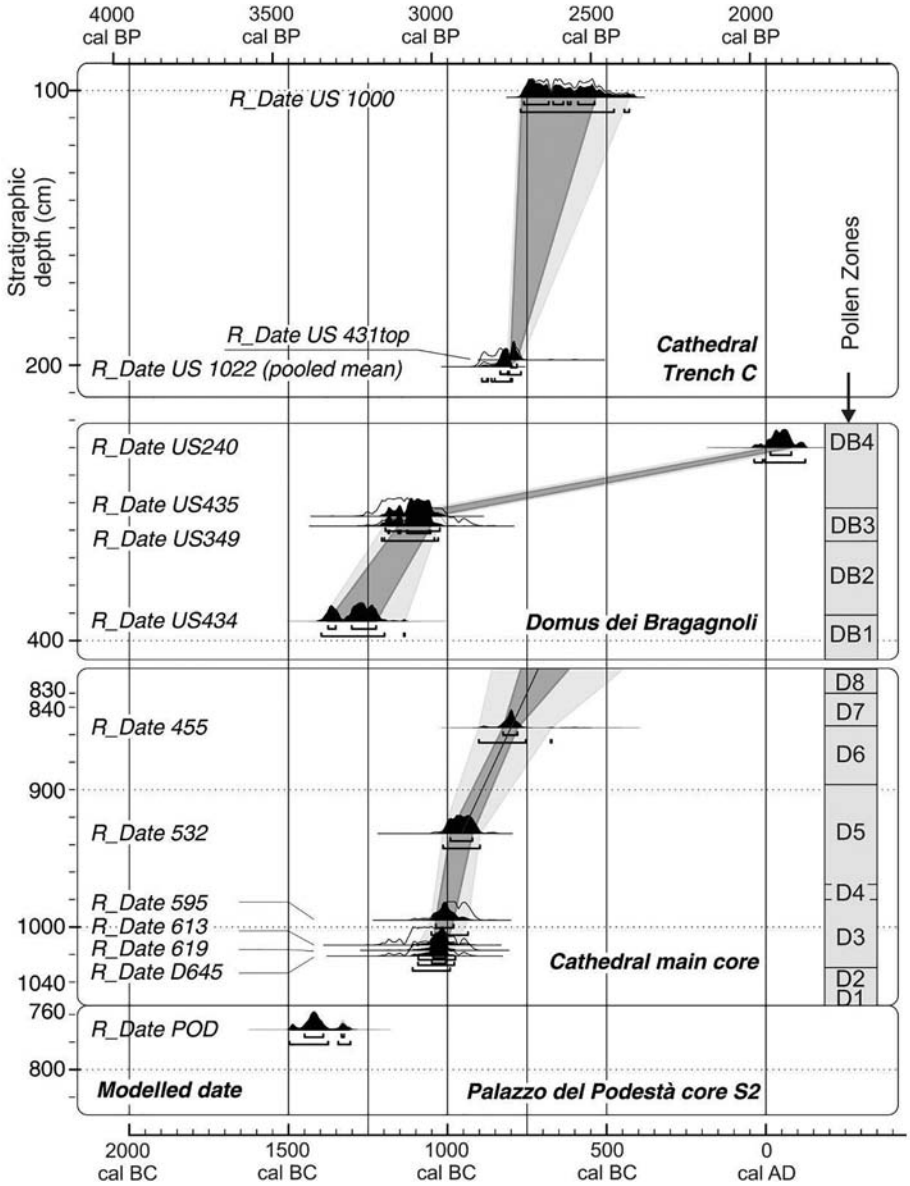

Fig. 9. Probability distributions of radiocarbon dates in the age–depth model of the four dated stratigraphic sequences (*Palazzo del Podestà* core S2, Cathedral main core, *Domus dei Bragagnoli* trench C, Cathedral trench C). For each of the modeled dates two distributions have been plotted: one in outline, which is the result of radiocarbon calibration, and a solid one, based on the chronological model. OxCal v4.3.2, Bronk Ramsey (2017); r:5 IntCal13 atmospheric curve (Reimer et al., 2013). For pollen zones see Figs. 10 and 11.

(lithofacies L3 and L4, see Fig. 6c; pollen zones D2 and D4 at site 1). Here, a bias to pollen associations is shown by low concentration and diversity, with an abnormal increase of pine pollen (Fig. 11), the latter is known to be resistant to leaching (Havinga, 1984). Therefore, zones D2 and D4 will not be considered in the hereafter paleoecological interpretation.

The charcoal fragments retrieved at 671 cm depth in the *Palazzo del Podestà* core S2 (Fig. 7) yielded the oldest age so far available from the stratigraphic successions drilled in the hearth of the hilltop town of Bergamo (Ub 40490 – modeled calibrated age 3355 ± 96 yrs. cal BP, i.e., 1405 yrs. cal BC, Suppl. Table S4). The pollen spectra from the same stratigraphic level thus provides a picture of Middle Bronze Age paleoenvironments on the Bergamo Hill. Early agropastoral activities are documented by pollen of cereals (0.2% of the pollen sum), *Ranunculus acris* type (1.4%), *Plantago lanceolata* (1.7%) and *P. media* type (0.3%). Pollen of trees and shrubs reaches 76% of the pollen sum (pie chart, Fig. 7), mostly represented by hygro-mesophilous deciduous forest *taxa* such as *Alnus glutinosa* type (20.9%), *Corylus* (33.9%), *Betula* (7.9%) and deciduous species of the genus *Quercus* (6.5%), accompanied by *Fagus* and *Carpinus betulus*. Pollen-slide charcoal concentration suggests limited fire activity. These paleoecological data speak for a limited, although present, human impact on extralocally forested landscape. Deposition occurred in an off-site position, i.e., with no sign of human activity in the deposition processes.

The following tile in the paleoenvironmental history of the Bergamo Hill comes from the nearby *Domus dei Bragagnoli* (Fig. 8b, 10). Here, stratigraphic units at the base of trench C yielded a calibrated age of 3233 yrs. cal BP (1283 yrs. cal BC, median probability of UBA 19904). The lowermost pollen zone DB1 (Fig. 10) points to the development of anthropized environments with cereal fields and pastures during the early decades of the Late Bronze Age. Sediments still document the presence of hygro-mesophilous deciduous forests, with woody species summing up to 60% of the pollen sum. Pie charts (Fig. 10) suggest a substantial stability between the plant ecological groups described for the Middle Bronze Age of *Palazzo del Podestà* core S2 and pollen zone DB1, apart from a visible reduction of shrubs (mostly related to *Corylus*) and an increase in total grass pollen.

The *Domus dei Bragagnoli* paleoecological record shows a major drop in AP values during zone DB2, from 75 to 25% of the pollen sum (Fig. 10). We have to keep in mind that this sequence formed in a near-site position type A (sensu Edwards, 1991; Ravazzi et al., 2019), implying that deposition was driven by anthropic processes (dumping, middening), and that its stratigraphic continuity is interrupted by anthropic cuts. We carefully use the available ^{14}C ages to constrain in time such drop in AP values. The AP fall and the development of anthropogenic habitats recorded in zone DB2 is to be set between 3233 yrs. cal BP (i.e., 1283 yrs. cal BC, median probability) and 3034 yrs. cal BP (i.e., 1084 yrs. cal BC, median probability). The latter is the mean radiocarbon age obtained pooling the ^{14}C ages of 2885 ± 47 and 2908 ± 29 yrs. uncal BP, which are statistically the same at 95% level of confidency. The *Domus dei Bragagnoli* sequence does not clear if the AP drop was a gradual or instead an abrupt process, given the stratigraphic peculiarities of the analyzed section. Unfortunately, the discussed drop in AP values is not visible in the Cathedral main core record, starting only at 2984 + 70/−37 yrs. cal BP (modeled age, 11th century BC, Fig. 11).

During the Final Bronze Age up to the beginning of the Iron Age (1200–800 yrs. cal BC; De Marinis, 2014), paleoecological data from both the Cathedral main core (pollen zones D1, D3, D5–D7, 2980–-2700 yrs. cal BP, 1030–750 yrs. cal BC) and *Domus dei Bragagnoli* (pollen zone DB3) document extensive activities related to a human settlement on the hilltop of Bergamo (Figs. 10–11). The area occupied by the agropastoral land dominated the Bergamo Hill, as documented by pollen of specific anthropogenic plants (Iversen, 1941, 1949) connected to human activities or quantitatively increasing in phase with the anthropic interference on the landscapes. Increasing charcoal concentration points to enhanced on-site fire activities (Fig. 13, panel 1), correlated to increasing anthropization. Crop fields, domestic gardens, vineyards, and pastures are documented by diagnostic pollen types of cultivated plants and of secondary anthropogenic indicators, such as cereals (0.4–6.4% of the pollen sums), scattered single pollen grains of *Linum usitatissimum* type, *Vitis* (0.2–1.5%),*Vicia* type (0.1–1.5%), *Plantago lanceolata* (0.6–3.7%) and *P. media* type (max 0.7%), *Orlaya grandiflora* type (0.2–2.9%), and *Malva*, *Convolvulus*, *Verbena*, *Centaurea cyanus*, etc. These plants have low pollen productivity (Turner and Brown, 2004; Denisow, 2011) and limited dispersal capability, thus their pollen might indicate the local occurrence of the plants into a radius of few tens-hundred meters around the studied area. Among those low producers, it is worth mentioning the continuous occurrence of *Vitis* pollen with values >1% in zone D5 (around 2900 yrs. cal BP, 10th century BC), confirmed by a record of pipe fragments dated to 2780 yrs. cal BP (median probability, i.e., 830 yrs. cal BC, see Section 5.3). The Bergamo Hill is far from the native habitat of *Vitis vinifera* subsp. *sylvestris* in N-Italy, i.e., riverside and gallery alluvial forests (Turner and Brown, 2004; Castellano et al., 2017), thus we may argue for grapevine cultivation uphill on the southern Alpine fringe as early as the 10th century BC, well before the onset of the Etruscan trades in the 6th century BC (Sassatelli and Govi, 2014).

5.2. Coprophilous spores and nutrients

Subsistence economy in the Final Bronze Age community on the hilltop of Bergamo relied not only on plant resources but also on livestock, whose traces are found in both stratigraphic sequences in the form of spores of coprophilous fungi (*Sordaria* type, *Sporormiella*, *Podospora*, *Delitschia*, *Tricodelitschia*, *Cercophora*, *Apiosordaria*, *Arnium*; Cugny et al., 2010; Feeser and O'Connell, 2010) and intestinal parasites (*Trichuris*, Brinkkemper and van Haaster, 2012). Such proxies are found in almost all the analyzed samples and are especially abundant and diverse in the Cathedral main core succession (Fig. 11), suggesting that animal droppings and their parasites were conveyed in this footslope area by runoff and atmospheric processes. The concentration of P (phosphorus) forms (Fig. 11) points in the same direction. Available and total P concentrations (expressed as mg/kg of sediment) steadily increase from pollen zone D1 to D3, settling then on high and stable values up to the end of the Bronze Age. These data indicate a continuous and conspicuous supply of nutrients in the sedimentary environment, and originating from animal manure (Sharpley and Moyer, 2000).

5.3. Fruits and seeds

A few cereals and pulses finds, attested by the analysis of plant macroremains carried out in layers associated with pollen zone DB3 in *Domus dei Bragagnoli* trench C, confirm human activities in a narrow range area. Furthermore, plant macroremains retrieved in Cathedral trench C deep layers (2780 yrs. cal BP, i.e., 830 yrs. cal BC) corresponding to pollen zone D7 of the Cathedral main core, besides a diversified crop spectrum (*Hordeum vulgare, Triticum monococcum, T. dicoccum, T. spelta, T.* cf. *timopheevi, Panicum miliaceum, Lens culinaris, Pisum sativum, Vicia faba* var. *minor, V.* cf. *sativa, Vitis vinifera*), indicate a high variety of habitats in the surroundings. Grapevine remains consist of two pipe fragments which attribution to domesticated forms remain uncertain. Most of the identified species refer to open habitats more or less intensively affected by human activities. Weeds of arable land, as well as gardens and grapevine cultivation, are documented. Some of these species, e.g., *Chenopodium album*, *Polygonum aviculare*, etc., might also grow in disturbed areas in the environments surrounding the settlements where soils were richer in nutrient and the competition was lower comparing with farmed land densely sown by cultivated plants. The other grassland communities, represented by plant macroremains, are discriminated by the different degree of soil humidity. Plant species favoring nutrient-rich, wet and deep mud as living substrate might grow in

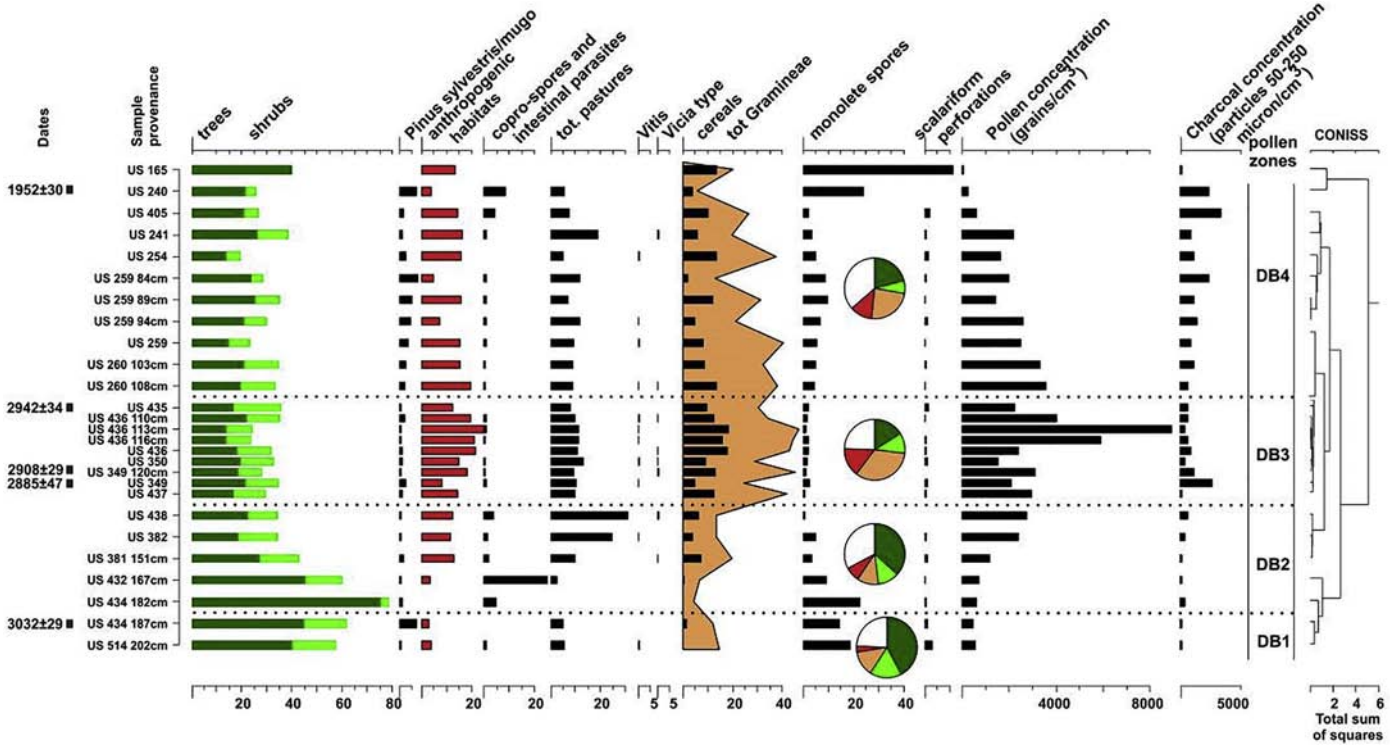

Fig. 10. *Domus dei Bragagnoli* trench C, uncalibrated ages, stratigraphic identification (SU, see Fig. 8b), paleoecological proxies for pollen taphonomy, land use, nutrient sinks and ecosystem structure. Keys to pollen pie charts in Fig. 7.

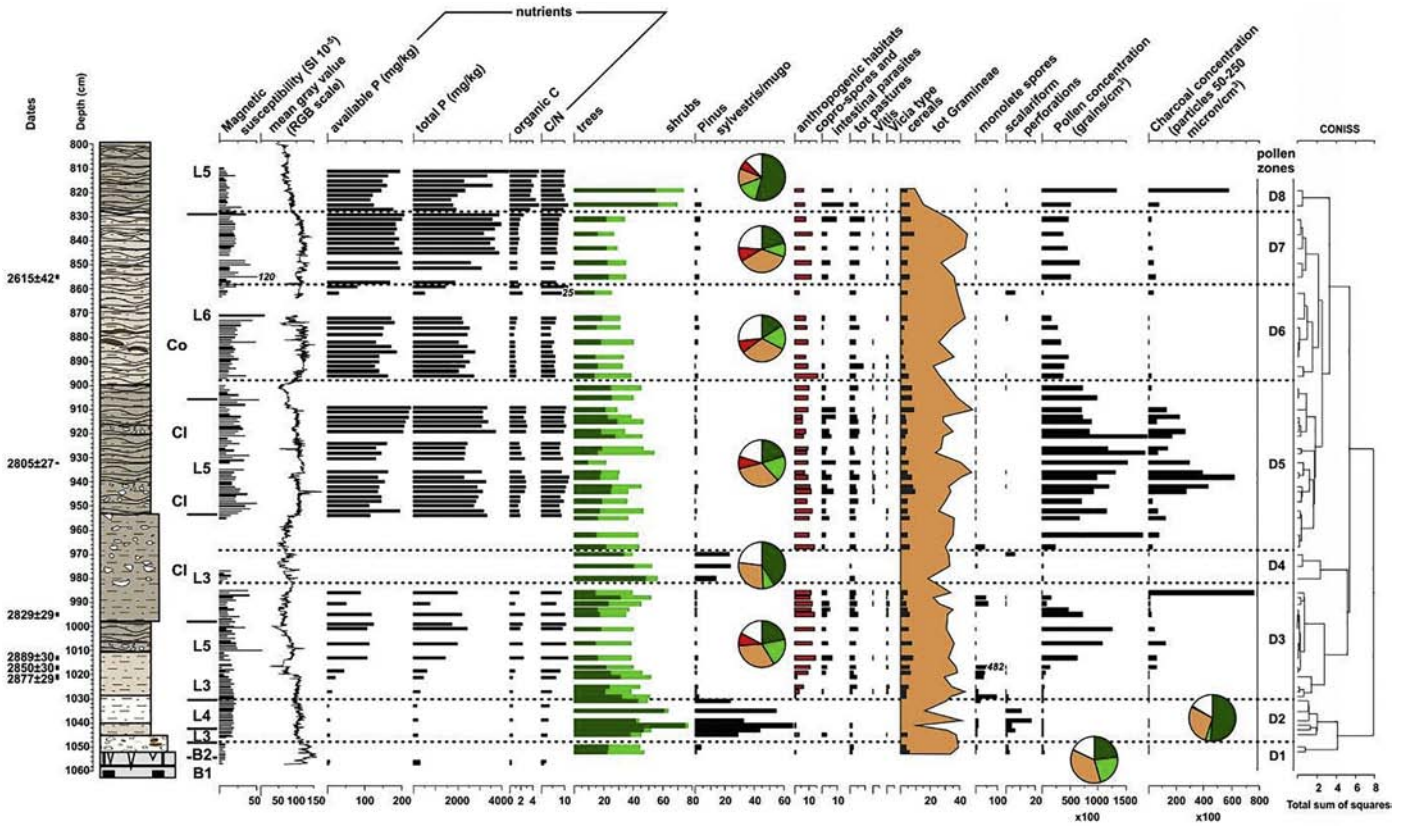

Fig. 11. Stratigraphy of the lower segment of the Cathedral main core showing uncalibrated ages, selected sedimentary and paleoecological proxies for pollen taphonomy, land use, nutrient sinks and ecosystem structure. Keys to stratigraphic log and pollen pie charts in Fig. 7.

depressed areas with low drainage, as well as in proximity of the springs or at the pond borders, e.g., *Epilobium palustre*. On the other hand, finds of *Hieracium* cf. *pilosella* indicate dry grasslands suffering from water deficit in summer season, e.g., on thin rocky soils covering the steep slopes strip by forest vegetation and affected by animal husbandry.

5.4. Wood charcoal identification

Wood charcoal data from *Domus dei Bragagnoli* trench C supports the presence of a hygro-mesophilous deciduous woodland in the surroundings of the ancient settlement, exploited by the site's inhabitants for firewood purposes. The anthracological record from the layers associated with the pollen zones DB2 (3 samples, 21 charcoal fragments) and DB3 (5 samples 88 charcoal fragments) is, in fact, strongly dominated be deciduous oaks (*Quercus spp*. deciduous; 15 fragments from DB2, 64 fragments from DB3) charcoal, with sporadic attestation of alder (*Alnus spp*.; 1 fragment from DB2) and beech (*Fagus sylvatica*; 1 fragment from DB2, 4 from DB3). The latest layers here considered, coeval to pollen zone DB3, are characterized by a relatively abundant (11 fragments) attestation of Rosaceae (*Prunus* sspp.) charcoal, which may support palynological evidence of a further reduction of the woodland cover connected to expansions of clearings and associated vegetation.

5.5. Evidence for land use change around 2700 yrs. cal BP

The underground stratigraphies from the hilltop of Bergamo offer a further glance into later phases of the Early Iron Age. This later portion of the deposit will be further investigated in a subsequent step of our research. The uppermost pollen zone of the Cathedral main core paleoecological record (D8, Fig. 11) shows a clear recovery of woody cover, with the total percentages of trees and shrubs pollen almost doubling. The main taxa involved in the process are *Carpinus betulus*, *Corylus* and deciduous *Quercus* and, to a lesser extent, *Betula* and *Fagus*. Grass habitats and terrestrial herb communities (especially pastures) shrank, as synthetically shown by the uppermost pie chart and relevant pollen curves of Fig. 11. According to the age-depth model of the Cathedral main core sequence, the age of onset pollen zone D8 is modeled 2700 yrs. cal BP (750 yrs. cal BC, Fig. 9). The decline of pastures is mirrored by strongly decreasing values of available and total P and by C/N rise in the same samples, suggesting either land abandonment or land use change.

6. Paleoenvironmental spatial reconstruction on the Bergamo hilltop, around 2800 yrs. cal BP (9th century BC)

According to the quantitative paleoecological records so far developed in the subsurface of the Bergamo hilltop (sites 1 and 3), the agro-pastoral land dominated the relevant pollen source area (RSAP). At these sites, however, sedimentology suggests that pollen deposition was partly vehiculated by runoff floatation, thus restricting and altering the source area predicted by RSAP for pure airborne deposition. Still, RSAP is believed to extend well beyond the studied area and most probably over the entire Bergamo Hill (see Marquer et al., 2020) which experienced a state of overall forest contraction at the end of the Bronze Age (2850 yrs. cal BP, i.e., 900 yrs. cal BC). This figure is consistent with the regional record of pasture expansion, coeval to the development of settlement on other hilltops in the low-mountain fringe of the Italian Alps, at the onset of the Iron Age (Gobet et al., 2000; Poggiani Keller, 2016; Ravazzi and Pini, 2013). The surface ratio between pastures and crop fields (arative fields + fallow land) calculated using topographic suitability criteria (2:4) is apparently inconsistent with the ratio between Gramineae and cereal pollen (5.5:1 in Pollen Zones D3, D5, D7), suggesting instead seminatural grasslands and pastures to prevail over crop fields in RSAP (Vorren, 1986; Makohonienko et al., 1998). It might be argued that a significant pasture development affected RSAP sunny slopes on the southern side of the Bergamo Hill, outside of the studied area. On the other hand, however, the extremely biodiverse record of dry pasture plants of low pollen productivity and limited dispersal capability speaks for their local occurrence close to sites 1 and 3 (Section 5). This hypothesis is corroborated by intensive runoff processes, activity of colluvial fans (Fig. 12), coprophilous spores abundance, and high phosphorus input at both sites. High stocking rate triggers significant upslope soil denudation and habitat diversification, with expansion of several different grassland types on calcareous parent material, either nutrient-demanding, basiphilous xerophytic, or acidophilous (Oberdorfer, 1977; Ellenberg, 1988; Poschlod et al., 1998). A water reservoir was exploited at site 1, providing an essential resource to animal husbandry. Due to low bedrock permeability and high summer precipitation, it is likely that more springs could be exploited for animal watering on the northern slope of the Bergamo Hills. It is likely that a number of springs, known to have been caught in the Roman Age on the northern side of the Bergamo Hills (see Fortunati and Ghiroldi, 2019), were already exploited in earlier times.

7. Synthesis, climate and cultural correlations

The analysis of sedimentary archives underlying the modern city of Bergamo provided new and unprecedented evidence on the Late Holocene land-use history and in connection to the emergence of an early settlement in the Late Bronze Age, before the development of the urban center, archeologically documented in the end 6th century BC (around 2500 yrs. cal BP).

Due to their depressed footslope position, the studied records offer a high degree of stratigraphic continuity. From this uninterrupted deposition it is possible to reconstruct an increasing of agropastoral activity coupled by a decrease of the seminatural forest cover, without an apparent chronological interruption between 3355 and before 2980 yrs. cal BP (median probabilities of modeled ages, i.e., 1405 and 1030 yrs. cal BC). The maximum intensity of human pressure is recorded from 2980 (or before) to around 2700 cal yrs. BP, as recorded by a drilling intercepting the infill sequence of a watering pond used for animal husbandry. The interdisciplinary study of these laminated natural deposits and coeval middens and dumps near-site to a settlement allowed to reconstruct the associated paleoenvironment during the 9th century BC. A state of overall forest reduction affected the Bergamo Hill in the Final Bronze Age and at the onset of the Iron Age. Those processes of farming expansion and woodland reclamation saw an end at around 2700 yrs. cal BC (750 yrs. cal BC), with a phase of generalized decline of agropastoral activities.

The cultural framework and the centennial-scale climatic constrains to this narrative are presented in Fig. 13, to highlight some potential correlations worthwhile of consideration:

(a) The cultural scenario – The development of the Golasecca culture in W-Lombardy, to which the earliest Bronze Age archeological assemblages from the Bergamo Hill are also referred (Poggiani Keller, 2016), is characterized by strong cultural continuity from the Late Bronze Age to the Iron Age (De Marinis, 2014). This recognition agrees with the long-term agropastoral development observed on the Bergamo Hill in the present study, showing interrupted occupation and land-use continuity starting in the Late Bronze Age and continuing for at least five centuries.

(b) The Alpine climatic oscillations – The phase of intensification of agropastoral impact on the Bergamo Hill, spanning the period between 3355 to around 2700 cal yrs. (13th–9th century BC), started in the "Late Bronze Age optimum," 3350–3100 yrs. cal BP (Fig. 13) described in the Alps from radiocarbon evidences of glacier retreat (Holzhauser, 1984) and characterized by land-use intensification (Tinner et al., 2003); while the decrease observed around 2700 yrs. cal BP occurred within, or lagged, the culmination of the "Early Iron Age cold phase," also known as Göschenen I event (Zoller et al., 1966), a today renowned Alpine event, recognized in the glacier record (Orombelli and Pelfini, 1985; Baroni and Carton, 1988; Deline and Orombelli, 2005) and dendrochronologically dated to 2752–2550 yrs. cal BP (802–608 yrs. cal BC, Le Roy et al., 2015). Globally, this phase is marked by a sudden increase

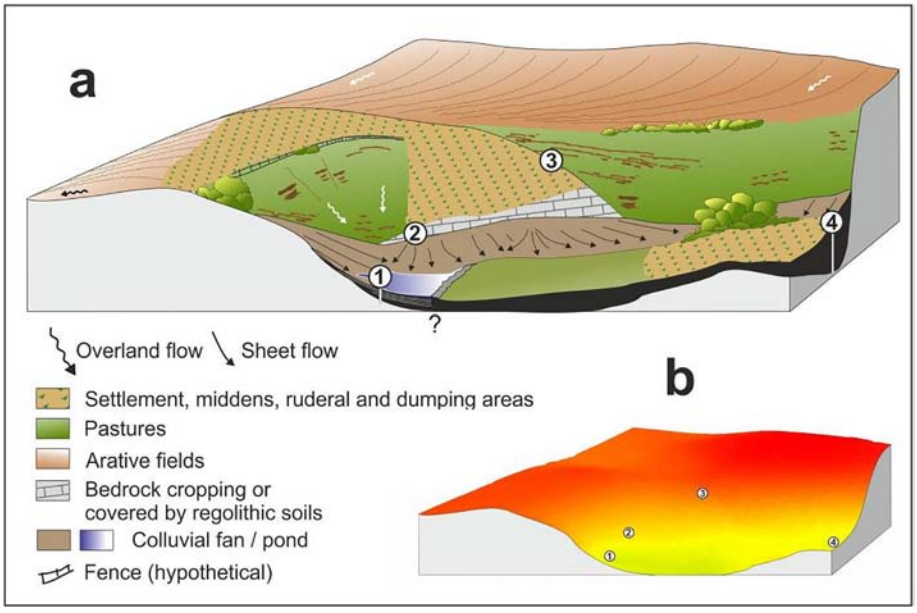

Fig. 12. Paleoenvironmental reconstruction of the studied area on the Bergamo hilltop around 2800 yrs. cal BP (i.e., 9th century BC, onset of the Iron Age). (a) Final reconstruction showing land use units, settlement areas and active geomorphic processes recognized from sedimentary archives 1–4 (Fig. 3) and supported by the available archeological record. (b) NW-view of the bedrock topography cut along the section A–B which served to build the reconstruction (see Fig. 3).

of atmospheric radiocarbon production which may have been driven by temporary declines of solar activity (van Geel et al., 1996, 1999; Mauquoy et al., 2004). The archeological record might also fit this figure, in that a phase of contraction has been envisaged in the 8th–6th century BC before the development of the Celtic center on the Bergamo hilltop (Poggiani Keller, 2016). Furthermore, the ceramic record of the Celtic

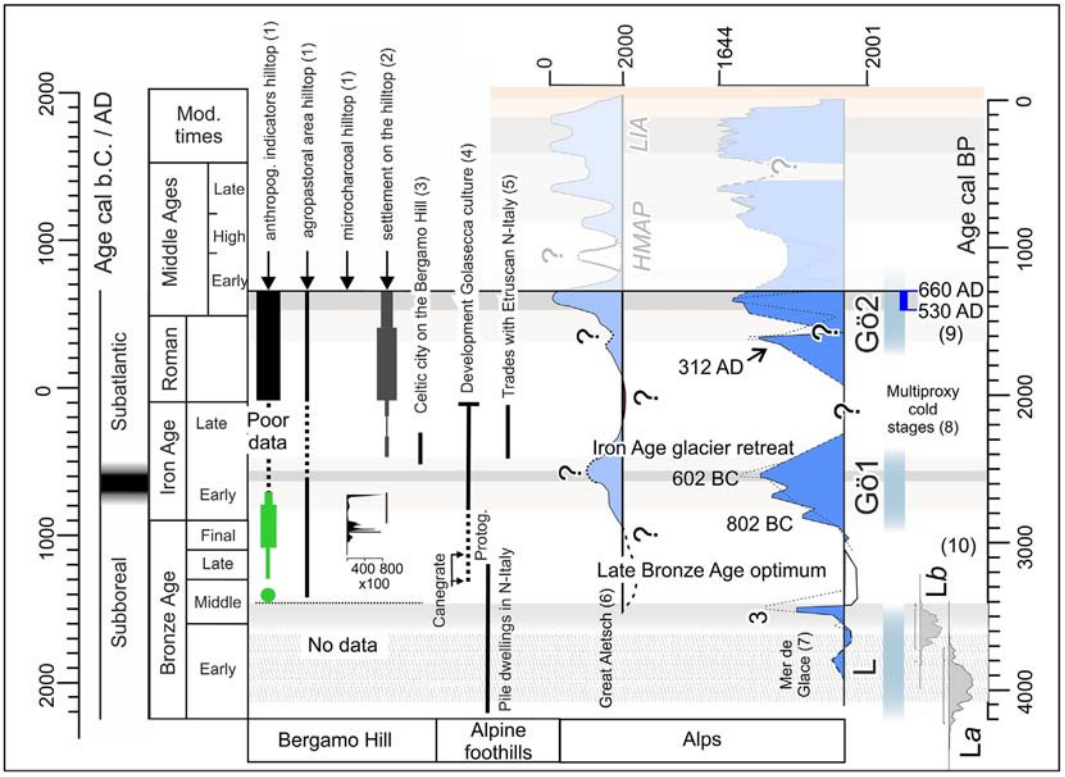

Fig. 13. Chronostratigraphic framework of regional cultural development and of centennial-scale climate constrains for the early environmental history and human settlement of the Bergamo Hill. The panel focuses the interval 4000–2000 yrs. cal BP. The Subboreal/Subatlantic boundary is from van Geel et al. (1996). (1) This paper – in green steps in development of agropastoral land; in black settlement structures; (2) Artifacts: Fortunati, 2012, Poggiani Keller, 2016; (3) Poggiani Keller, 2001; (4) Chronology of cultural development in W-Lombardy, N-Italy, from the Late Bronze Age to the Early Iron Age, De Marinis, 2009, 2014; (5) Sassatelli and Govi, 2014; (6) Glacier advances of the Great Aletsch, the major glacier of the Alps; Holzhauser, 1984; Holzhauser et al., 2005; here the "Late Bronze Age optimum" was constrained by peat evidence of glacier retreat; (7) Glacier advances of the Mer de Glace (Mont Blanc), from Le Roy et al., 2015; (8) Göschenen cold periods after Zoller et al., 1966; Patzelt and Bortenschlager, 1973; Badino et al., 2018; (9) Dendroclimatology by Büngten et al., 2005; Büntgen et al., 2011. (10) Löbben cold phase (La and Lb): Calibration intervals for ages 3576 (median) ± 140 yrs. cal BP and 3811 (median) ± 180/−203 yrs. cal BP dating the type section in Eastern Alps (Patzelt and Bortenschlager, 1973) (For interpretation of the references to color in this figure legend, the reader is referred to the web version of this article.)

urban settlement post-dates the 7th century BC (>2550 yrs. cal BP), while the city reached its maximum extent around 500 yrs. cal BC (Poggiani Keller, 2001), fitting a warm phase subsequent to Göschenen I, with intensified land-use in the Alps (2600–2400 yrs. cal BP, i.e., 650–450 yrs. cal BC, Tinner et al., 2003). We are aware that such climate–cultural correlations do not imply causal relations per se, and that feedbacks between climate and socio-cultural systems may be complex (deMenocal, 2001; Rosen, 2007). Further work is needed to develop independent climatic proxies and associated chronologies both from the natural archives and from on-site records. We are also warning about the incompleteness of the archeological record so far published. Indeed, lack of archeological evidence in the 8th–6th century BC is not a conclusive evidence for absence of settlement continuity.

8. Conclusion

While investigating the origin and early history of European modern cities, the study of natural archives hidden under a thick pile of urban deposits can yield invaluable information for both Quaternary paleoecologists and archeologists. These layers, archeologically sterile, lacking any macroscopic sign of occupation, are often located near-site to agropastoral settlements, forerunners of the later urban centers, unpredicted by archeological evidence. Microbotanical and sedimentary evidence in off-site and near-site location to unpredicted ancient settlements provides an array of proxies for quantitative reconstruction of human land use intensity and its diachronic change, which ultimately allows to reconstruct the first occurrence of human settlements themselves.

Author contributions

C.R. designed the work. M.D. carried out spatial elaborations. C.R. and D.M. built the age-depth models. R.Pi. and G.F. performed palynological, pollen charcoal and magnetic susceptibility analysis; R.C. and D.A.E.K. performed biogeochemical analysis; R.Pe. studied fruits and seed associations, L.C. carried out anthracological identifications. C.R., R.P., R.Pe and L.C. wrote the paper. Photographs and artwork were realized by C.R., R.P., M.D. All authors shared the ideas of the paper, discussed the multidisciplinary environmental reconstruction, and reviewed earlier drafts of the manuscript.

Declaration of Competing Interests

The authors declare that they have no known competing financial interests or personal relationships that could have appeared to influence the work reported in this paper.

Funding

This research did not receive any specific grant from funding agencies in the public, commercial, or not-for-profit sectors.

Acknowledgments

The study of archeological trenches was promoted by Soprintendenza per i Beni Archeologici della Lombardia. Specifically, the study of the *Domus dei Bragagnoli* trench C was undertaken under the direction of Dr. Maria Fortunati with the financial support by Impresa Pandini S.p.A.(Bergamo, Italy); contract n. 103, dated May 6, 2011; the study of the Cathedral trench C was carried out under the direction of Dr. Raffaella Poggiani Keller and with the generous help of the late Mr. Franco Magri. We want to express our gratitude to: Dr. Sergio Chiesa (CNR-IDPA) for inviting us to study the subsurface drillings in the Bergamo city; Fabio Baio, technical director of the studied drillings; Stefano Banfi (Dept. of Physics, University of Milano-Bicocca) for skillful longitudinal cutting of the heavy consolidated core cylinders of the Cathedral and *Palazzo del Podestà* cores; Camilla Croci (B.Sc. at CNR-IGAG) and Bernardo Raineri (B.Sc at Univ. Milano Bicocca) for their contribution to pollen and C/N analysis; Dr. Giovanni Monegato (CNR-IGG) for sedimentological advices and Dr. Stefania Casini (Museo Civico Archeologico, Bergamo) for archeological hints on an early version of this paper. This is a contribution to the CNR-IGAG research line DTA. AD001.112 – Quaternary paleoenvironments and palaleoclimate.

Appendix A. Supplementary data

Supplementary data to this article can be found online at https://doi.org/10.1016/j.revpalbo.2020.104205.

References

Badino, F., Ravazzi, C., Vallè, F., Pini, R., Aceti, A., Brunetti, M., Champvillair, E., Maggi, V., Maspero, F., Perego, R., Orombelli, G., 2018. 8800 Years of high-altitude vegetation and climate history at the Rutor Glacier forefield, Italian Alps. Evidence of Middle Holocene timberline rise and glacier contraction. Quat. Sci. Rev. 185, 41–68.

Barker, P., 1993. Techniques of Archaeological Excavation. Psychology Press, New York.

Baroni, C., e Carton, A., 1988. Vedretta di Pisgagna (Gruppo dell'Adamello). Geomorfologia e variazioni oloceniche della fronte. Natura Bresciana 26, 5–34.

Bersezio, R., Bini, A., Ferliga, C., Gelati, R., 2012. Note Illustrative Della Carta Geologica d'Italia alla Scala 1:50.000 - Foglio 098 Bergamo. Servizio Geologico d'Italia – Regione Lombardia.

Bersezio, R., Bini, A., Gelati, R., Ferliga, C., Rigamonti, I., Strini, A., 2013. Note Illustrative Della Carta Geologica d'Italia alla Scala 1:50.000 - Foglio 097 Vimercate. Servizio Geologico d'Italia – Regione Lombardia.

Beug, H.J., 2004. Leitfaden der Pollenbestimmung für Mitteleuropa und angrenzende Gebiete. Verlag Dr. Friedrich Pfeil, München, Germany.

Bonalumi, G., Roncalli, W., Vitali, G., 1992. I suoli dell'hinterland bergamasco. E.R.S.A.L. Progetto "Carta Pedologica", SSR 12, Milano, p. 106.

Brinkkemper, O., van Haaster, H., 2012. Eggs of intestinal parasites whipworm (*Trichuris*) and mawworm (*Ascaris*): Non-pollen palynomoprhs in archaeologial samples. Rev. Palaeobot. Palynol. 186, 16–21.

Bronk Ramsey, C., 2017. Methods for summarizing radiocarbon datasets. Radiocarbon 59 (2), 1809–1833.

Bronk Ramsey, C., Lee, S., 2013. Recent and planned developments of the program OxCal. Radiocarbon 55 (2-3), 720–730.

Büngten, U., Esper, J., Frank, D.C., Nicolussi, K., Schmidhalter, M., 2005. A 1052-year tree-ring proxy for Alpine summer temperatures. Clim. Dynam. 25, 141–153.

Büntgen, U., Tegel, W., Nicolussi, K., McCormick, M., Frank, D., Trouet, V., Kaplan, J.O., Herzig, F., Heussner, K.U., Wanner, H., 2011. 2500 Years of European climate variability and human susceptibility. Science 331, 578–582.

Cappers, R.T.J., Bekker, R.M., Jans, J.E.A., 2006. Digitale Zadenatlas van Nederland (Digital Seed Atlas of The Netherlands). Groningen Archaeological Studies 4Barkhuis Publishing, Eelde.

Casini, S., De Marinis, R., Rapi, M., 2001. L'abitato protostorico nei dintorni di Como. La protostoria in Lombardia. Atti 3° Convegno Archeologico Regionale, Como, pp. 97–158.

Castellano, L., Ravazzi, C., Furlanetto, G., Pini, R., Saliu, F., Lasagni, M., Orlandi, M., Perego, R., Degano, I., Valoti, F., De Marinis, R.C., Casini, S., Quirino, T., Rapi, M., 2017. Charred honeycombs discovered in Iron Age Northern Italy. A new light on boat beekeeping and bee pollination in pre-modern world. J. Archaeol. Sci. 83, 26–40.

Chiesa, S., Pini, R., 2008. Lo sviluppo della città e le trasformazioni morfologiche e paleoambientali del Colle di Bergamo. In: Zoppetti, Maria Mencaroni (Ed.), D'erbe e piante adorno. Ateneo di Scienze, Lettere e Arti di Bergamo. Fondazione per la Storia Economica e Sociale di Bergamo, pp. 127–140.

Metodi di analisi chimica del suolo. In: Colombo, C., Miano, T.M. (Eds.), 3a versione, SISS. Pubblicità e Stampa, Bari.

Crespi, A., Brunetti, M., Lentini, G., Maugeri, M., 2018. 1961-1990 high-resolution monthly precipitation climatologies for Italy. Int. J. Climatol. 38, 878–895.

Cugny, C., Mazier, F., Galop, D., 2010. Modern and fossil non-pollen palynomorphs from the Basque mountains (western Pyrenees, France): The use of coprophilous fungi to reconstruct pastoral activity. Veg. Host. Archeobot. 19, 391–408.

Cushing, E.J., 1967. Evidence for differential pollen preservation in Late Quaternary sediments in Minnesota. Rev. Palaeobot. Palynol. 4, 87–101.

De Marinis, R.C., 2009. Continuity and discontinuity in Northern Italy from the recent to the final Bronze Age: A view from North-Western Italy. Sci. dell'Antichità Storia Archeol. Antropol. 15, 535–545.

De Marinis, R.C., 2014. Correlazioni cronologiche tra Italia nord-occidentale (Area della Cultura di Golasecca) e ambiti culturali transalpini e cisalpini dal Bronzo Recente alla fine del VII secolo a.C. Les Celtes et le Nord de l'Italie (Premier et Second Âges du fer). Actes du XXXVIe colloque international de l'A.F.E.A.F. (Vérone, 17-20 mai 2012) 17, 17–36 (36e supplément à la R.A.E.).

Dearing, J., 1999. Magnetic susceptibility. In: Walden, J., Oldfied, F., Smith, J.P. (Eds.), Environmental Magnetism: A Practical Guide. Technical Guide No. 6. Quaternary Research Association, London, pp. 35–62.

Deline, P., Orombelli, G., 2005. Glacier fluctuations in the western Alps during the Neoglacial, as indicated by the Miage morainic amphitheatre (Mont Blanc massif, Italy). Boreas 34 (4), 456–467.

deMenocal, P.B., 2001. Cultural responses to climate change during the Late Holocene. Science 292, 27.
Denisow, B., 2011. Pollen production of selected ruderal plant species in the Lublin area. University of Life Sciences in Lublin Press, p. 86.
Edwards, K.J., 1991. Using space in cultural palynology: The value of the off-site pollen record. In: Harris, D.R., Thomas, K.D. (Eds.), Modelling Ecological Change. Institute of Archaeology. University College London.
Ellenberg, H., 1988. Vegetation Ecology of Central Europe. Fourth Ed. Cambridge University Press, Cambridge, p. 751.
Feeser, I., O'Connell, M., 2010. Late Holocene land-use and vegetation dynamics in an upland karst region based on pollen and coprophilous fungal spore analysis: An example from the Burren, western Ireland. Veg. Hist. Archeobot. 19, 409–426.
Fernández-Götz, M., 2015. Urban experiences in early Iron Age Europe: Central places and social complexity. Contrib. New World Archaeol. 9, 11–32.
Fohlmeister, J., Vollweiler, N., Spötl, C., Mangini, A., 2013. COMNISPA II: Update of a mid-European isotope climate record, 11 ka to present. Holocene 23 (5), 749–754.
Fornoni, E., 1890. Orografia di Bergamo e le mura antiche, le porte cittadine, le pusterle, Atti dell'Ateneo Bergamo 1889-1890, I-XCVI.
Fortunati, M., 2012. La città in età romana. In: Fortunati, M., Ghiroldi, A. (Eds.), Hospitium Comunis Pergami. Scavo archeologico, restauro e valorizzazione di un edificio storico della città, pp. 57–59.
Fortunati, M., Ghiroldi, A., 2019. Il sistema di distribuzione delle acque in Città Alta in età Romana: acquedotti e cisterne. In: Casini, S., Fortunati, M., Poggiani Keller, R. (Eds.), Bergomum. Un colle che divenne città, pp. 179–185.
Furlanetto, G., Ravazzi, C., Pini, R., Vallè, F., Brunetti, M., Comolli, R., Novellino, M.D., Garozzo, L., Maggi, V., 2018. Holocene vegetation history and quantitative climate reconstructions in a high-elevation oceanic district of the Italian Alps. Evidence for a middle to late Holocene precipitation increase. Quat. Sci.Rev. 200, 212–236.
Gedye, S.J., Jones, R.T., Tinner, W., Ammann, B., Oldfield, F., 2000. The use of mineral magnetism in the reconstruction of fire history: A case study from Lago di Origlio, Swiss Alps. Palaeogeogr. Palaeoclimatol. Palaeoecol. 164 (1–4), 101–110.
Gelati, R., Passeri, L.D., 1967. Il Flysch di Bergamo, nuova formazione cretacica delle Prealpi Lombarde. Riv. It. Paleont. Strat. 73 (3), 835–849.
Ghiroldi, A., 2019. Dalla Cattedrale alle Domus: a ritroso nel tempo. In: Casini, S., Fortunati, M., Poggiani Keller, R. (Eds.), Bergomum. Un colle che divenne città, pp. 211–213.
Gobet, E., Tinner, W., Hubschmid, P., Jansen, I., Wehrli, M., Ammann, B., Wick, L., 2000. Influence of human impact and bedrock differences on the vegetational history of the Insubrian Southern Alps. Veget. Hist. Archaeobot. 9, 175–178.
Grimm, E.C., 2015. Tilia/tgview 2.0.41. Illinois State Museum, Research and Collections Center, Springfield, IL.
Havinga, A.J., 1984. A 20-year experimental investigation into the differential corrosion susceptibility of pollen and spores in various soil types. Pollen Spores 26, 541–558.
Holzhauser, H., 1984. Zur Geschichte der Aletschgletscher und des Fiescher-gletschers. Physische Geographie vol. 12 Zürich.
Holzhauser, H., Magny, M., Zumbühl, H.J., 2005. Glacier and lake-level variations in west-central Europe over the last 3500 years. Holocene 15 (6), 789–801.
Hosch, S., Zibulski, P., 2003. The influence of inconsistent wet-sieving procedures on the macroremains concentration in waterlogged sediments. J. Archaeol. Sci. 30, 849–857.
Iversen, J., 1941. Landnam i Danmarks stenalder. En pollenanalytisk undersøgelse over det første landbrug indvirkung paa vegetationsudviklingen (=Danmarks Geol. Unders. II.R., 66). København.
Iversen, J., 1949. The Influence of Prehistoric Man on Vegetation. Danmarks Geologiske Undersøgelse vol. 4. Reitzel, Copenhagen.
Jacobsson, P., Hamilton, W.D., Cook, G., Crone, A., Dunbar, E., Kinch, H., Naysmith, P., Tripney, B., Xu, S., 2018. Refining the Hallstatt Plateau: Short-term ^{14}C variability and small-scale offsets in 50 consecutive single tree-rings from southwest Scotland dendro-dated to 510–460 BC. Radiocarbon 60, 219–237.
Jacomet, S., 2006. Bestimmung von Getreidefunden aus archäologischen Ausgrabungen. 2. Auflage (1. Auflage 1987). Hrsg. vom IPNA. Universität Basel/Identification of cereal remains from archaeological sites, 2nd edition (1st ed. 1987) Published by the IPAS, Basel University.
Jacquiot, C., Trenard, Y., Dirol, D., 1973. Atlas d'Anatomie des Bois des Angiosperms. Centre Technique du Bois, Paris.
Jones, A.P., Tucker, M.E., Hart, J.K., 1999. The description and analysis of Quaternary stratigraphic field sections. Technical Guide No. 7Quaternary Research Association, London, p. 295.
Jordanova, N., Petrovsky, E., Kovacheva, M., Jordanova, D., 2001. Factors determining magnetic enhancement of burnt clay from archaeological sites. J. Archaeol. Sci. 28 (11), 1137–1148.
Lanza, M., 2003. Ricostruzione tridimensionale del sottosuolo della parte est della città di Bergamo. Tesi di Laurea in Scienze della Terra. Università degli Studi di Milano (A.A. 2002–2003).
Laporte, L.F., Behrensmeyer, A.K., 1980. Tracks and substrate reworking by terrestrial vertebrates in Quaternary sediments of Kenya. J. Sediment. Res. 50 (4), 1337–1346.
Le Roy, M., Nicolussi, K., Deline, P., Astrade, L., Edouard, J.L., Miramont, C., Arnaud, F., 2015. Calendar-dated glacier variations in the western European Alps during the Neoglacial: The Mer de Glace record, Mont Blanc Massif. Quat. Sci. Rev. 108, 1–22.
Ledger, P.M., Miras, Y., Poux, M., Milcent, P.Y., 2015. The palaeoenvironmental impact of prehistoric settlement and proto-historic urbanism: Tracing the emergence of the Oppidum of Corent, Auvergne, France. PLos One https://doi.org/10.1371/journal.pone.0121517 April 8, 2015.
Lees, J., 1999. Evaluating magnetic parameters for use in source identification, classification and modelling of natural and environmental materials. In: Walden, J., Oldfied, F., Smith, J.P. (Eds.), Environmental Magnetism: A Practical Guide. Technical Guide No. 6. Quaternary Research Association, London, pp. 113–138.
Makohonienko, M., Gaillard, M.J., Tobolski, K., 1998. Modern pollen/land use relationships in ancient cultural landscapes of north-western Poland, with an emphasis on mowing, grazing, and crop cultivation. In: Gaillard, M.J., Berglund, B.E. (Eds.), Quantification od land surfaces cleared of forests during the Holocene – Modern pollen/vegetation/landscape relationships as an aid to the interpretation of fossil pollen data. European Palaeoclimate and Man 18, pp. 85–101.
Marquer, L., Mazier, F., Sugita, S., Galop, D., Houet, T., Faure, E., Gaillard, M.J., Haunold, S., de Munnik, N., Simonneau, A., De Vleeschouwer, F., Le Roux, G., 2020. Pollen-based reconstruction of Holocene land-cover in mountain regions: Evaluation of the Landscape Reconstruction Algorithm in the Vicdessos valley, northern Pyrenees, France. Quat. Sci. Rev. 228, 106049. https://doi.org/10.1016/j.quascirev.2019.106049.
Mauel, S., Frame, D., Madison, F., 2013. Mapping bedrock: Models and field tools to identify loss potential in vulnerable landscapes. University of Wisconsin Discovery farms, Summer 2013. www.uwdiscoveryfarms.org.
Mauquoy, D., van Geel, B., Blaauw, M., Speranza, A., van der Plicht, J., 2004. Changes in solar activity and Holocene climatic shifts derived from ^{14}C wiggle-match dated peat deposits. The Holocene 14 (1), 45–52.
Mercuri, A.M., Montecchi, M.C., Pellacani, G., Florenzano, A., Rattighieri, E., Cardarelli, A., 2014. Environment, human impact and the role of trees on the Po plain during the Middle and Recent Bronze Age: Pollen evidence from the local influence of the terramare of Baggiovara and Casinalbo. Rev. Palaeobot. Palynol. 218 (1), 231–249.
Morellón, M., Anselmetti, F.S., Ariztegui, D., Brushulli, B., Sinopoli, G., Wagner, B., Sadori, L., Gilli, A., Pambuku, A., 2016. Human–climate interactions in the central Mediterranean region during the last millennia: The laminated record of Lake Butrint (Albania). Quat. Sci. Rev. 136, 134–152.
Neef, R., Cappers, R.T.J., Bekker, R.M., Boulos, L., 2012. Digital atlas of economic plants in archaeology. Groningen archaeological studies, 17Barkhuis Publishing, Eelde.
Nicolussi, K., Kaufmann, M., Patzelt, G., van derPlicht, J., Thurner, A., 2005. Holocene tree-line variability in the Kauner Valley, Central Eastern Alps, indicated by dendrochronological analysis of living trees and subfossil logs. Veg. Hist. Archaeobot. 14 (3), 221–234.
Ninfo, A., Fontana, A., Mozzi, P., Ferrarese, F., 2009. The map of Altinum, ancestor of Venice. Science 325, 577.
Oberdorfer, E., 1977. Süddeutsche Pflanzengesellschaften. Teil III. Wirtschaftswiesen und Unkrautgesellschaften. Fischer, Jena, p. 455.
Oldfield, F., 1999. Environmental magnetism; the range of application. In: Walden, J., Oldfied, F., Smith, J.P. (Eds.), Environmental Magnetism: A Practical Guide. Technical Guide No. 6. Quaternary Research Association, London, pp. 212–239.
Orombelli, G., Pelfini, M., 1985. Una fase di avanzata glaciale nell'Olocene superiore, precedente alla Piccola Glaciazione, nelle Alpi Centrali. Rend. Soc. Geol. It 8, 17–20.
Patzelt, G., Bortenschlager, S., 1973. Die postglazialen Gletscher- und Klimaschwankungen in der Venedigergruppe (Hohe Tauern, Ostalpen). Zeitschrift für Geomorphologie N.F. 16, 25–72 Suppl. Bd.
Pini R. et al., in preparation - Life on a hill top: vegetation history and land use at the dawn of the Bergomum settlement (northern Italy), XV to VI century BC.
Pini, R., Castellano, L., Perego, R., Ravazzi, C., Chiesa, S., De Amicis, M., Poggiani Keller, R., 2016. Nuovi dati sulla storia ambientale del centro abitato di Bergamo Alta tra la fase arcaica dell'età del Bronzo e il Medioevo. Stratigrafia, paleoecologia e archeobotanica dei depositi del Palazzo del Podestà (Piazza Vecchia). Atti dell'Ateneo di Scienze, Lettere, ed Arti, Bergamo LXXIX, pp. 349–371.
Poggiani Keller, R., 2001. Il centro protourbano di Bergamo e il sistema dei siti collinari coevi tra Oglio e Adda. La protostoria in Lombardia. Atti 3° Convegno Archeologico Regionale, Como, pp. 381–413.
Poggiani Keller, R., 2007. L'età del Ferro. Dall'oppidum degli Orobi alla formazione della città sul colle. In: Fortunati, M., Poggiani, R. (Eds.), Storia Economica e Sociale di Bergamo. I primi millenni Vol. 1, pp. 147–189.
Poggiani Keller, R., 2012. Il primo abitato sul colle: il centro protourbano dei Celti golasecchiani. In: Fortunati, M., Ghiroldi, A. (Eds.), Hospitium Comunis Pergami. Scavo archeologico, restauro e valorizzazione di un edificio storico della città, pp. 54–56.
Poggiani Keller, R., 2016. La scelta del sito della prima città. Atti dell'Ateneo Scienze Lettere ed Arti di Bergamo LXXIX, pp. 163–173.
Poschlod, P., Kiefer, S., Tränkle, U., Fischer, S., Bonn, S., 1998. Plant species richness in calcareous grasslands as affected by dispersability in space and time. Appl. Veget. Sci. 1, 75–90.
Punt, W., Blackmore, S. (Eds.), 1976-2009. The Northwest European Pollen Flora. vols. I-IX. Elsevier Publishing Company.
Ravazzi, C., Pini, R., 2013. Clima, vegetazione forestale e alpeggio tra la fine del Neolitico e l'inizio dell'Età del Bronzo nelle Alpi e in Pianura Padana. In: De Marinis, a cura di R. (Ed.), L'età del Rame. La Pianura Padana e le Alpi al tempo di Ötzi. Museo Diocesano di Brescia, Brescia, pp. 69–86.
Ravazzi, C., Marchetti, M., Zanon, M., Perego, R., Quirino, T., Deaddis, M., De Amicis, M., Margaritora, D., 2013. Lake evolution and landscape history in the lower Mincio River valley, unravelling drainage changes in the central Po Plain (N-Italy) since the Bronze Age. Quat. Int. 288, 195–205.
Ravazzi, C., Badino, F., Castellano, L., De Nisi, D., Furlanetto, G., Perego, R., Zanon, M., Dal Corso, M., De Amicis, M., Monegato, G., Pini, R., Vallé, F., 2019. Introduzione allo studio stratigrafico e paleoecologico dei laghi intramorenici del Garda. In: Baioni, a cura di M., Mangani, C., Ruggiero, M.G. (Eds.), Le Palafitte. Ricerca, Conservazione, Valorizzazione. Collana Palafitte/Palafittes/Pfahlbauten/Pile Dwellings/Palafitte. SAP – Società Archeologica, pp. 167–183.
Reille, M., 1992-1998. Pollen et spores d'Europe et d'Afrique du Nord. Laboratoire de Botanique historique et palynologie, Marseille.
Reimer, P.J., Bard, E., Bayliss, A., 2013. IntCal13 and Marine13 radiocarbon age calibration curves 0–50,000 years cal BP. Radiocarbon 55, 1869–1887.

Rentzel, P., Nicosia, C., Gebhardt, A., Brönnimann, D., Pümpin, C., Meyer, K.I., 2017. Trampling, poaching and the effect of traffic. In: Nicosia, C., Stoops, G. (Eds.), Archaeological Soil and Sediment Micromorphology. John Wiley & Sons Ltd, Chichester.
Rosen, A., 2007. Civilizing Climate: Social Responses to Climate Change in the Ancient Near East. Altamira Press, Plymouth, p. 209.
Sadori, L., Allevato, E., Bellini, C., Bertacchi, A., Boetto, G., Di Pasquale, G., Giachi, G., Giardini, M., Masi, A., Pepe, C., Russo Ermolli, E., Mariotti Lippi, M., 2015. Archaeobotany in Italian ancient Roman harbours. Rev. Palaeobot. Palynol. 218, 217–230.
Sassatelli, G., Govi, E., 2014. Etruria on the Po and the Adriatic. In: Turfa, J.M. (Ed.), The Etruscan World. Routledge, pp. 281–300.
Schoeneberger, P.J., Wysocki, D.A., Benham, E.C., Broderson, W.D., 1998. Field book for describing and sampling soils. Natural Resources Conservation Service USDA. National Soil Survey Center, Lincoln, NE.
Schweingruber, F.H., 1990a. Anatomie europaischer Holzer. Ein Atlas zur Bestimmung europäischer Baum-, Strauch- und Zwergstrauchhölzer. Verlag Paul Haupt, Bern und Stuttgart, p. 800.
Schweingruber, F.H., 1990b. Microscopic Wood Anatomy; Structural Variability of Stems and Twigs in Recent and Subfossil Woods from Central Europe. 3rd Ed. Eidgenössische Forschungsanstalt WSL, Birmensdorf.
Sharpley, A., Moyer, B., 2000. Phosphorous forms in manure and compost and their release during simulated rainfall. J. Environ. Qual. 29, 1462–1469.
Die Frage der Protourbanisation in der Eisenzeit. La question de la proto-urbanisation à l'âge du Fer. Akten des 34. internationalen Kolloquiums der AFEAF vom 13.–16. In: Sievers, S., Schönfelder, M. (Eds.), Mai 2010 in Aschaffenburg. Habelt, Bonn.
Stockmarr, J., 1971. Tablets with spores used in absolute pollen analysis. Pollen Spores 13, 615–621.
Strahler, A., Strahler, A., 2007. Physical Geography. Wiley India Pvt. Limited, p. 772.
Stuiver, M., Reimer, P.J., Reimer, R., 2013. Radiocarbon Calibration Program Revision 7.0.2.
Tinner, W., Lotter, A.F., Ammann, B., Conedera, M., Hubschmid, P., van Leeuwen, J.F.N., Wehrli, M., 2003. Climatic change and contemporaneous land-use phases north and south of the Alps 2300 BC to 800 AD. Quat. Sci. Rev. 22, 1447–1460.
Turner, S.D., Brown, A.G., 2004. *Vitis* pollen dispersal in and from organic vineyards. I. Pollen trap and soil pollen data. Rev. Palaeobot. Palynol. 129, 117–132.
van Geel, B., Buurman, J., Waterbolk, H.T., 1996. Archaeological and palaeoecological indications of an abrupt climate change in The Netherlands, and evidence for climatological teleconnections around 2650 BP. J. Quat. Sci. 11 (6), 451–460.
van Geel, B., Raspopov, O.M., Renssen, H., van der Pflicht, J., Dergachev, V.A., Meijer, H.A.J., 1999. The role of solar forcing upon climate change. Quat. Sci. Rev. 18 (3), 331–338.
Vorren, K.-D., 1986. The impact of early agriculture on the vegetation of Northern Norway. A discussion of anthropogenic indicators in biostratigraphical data. In: Behre, K.-E. (Ed.), Anthropogenic Indicators in Pollen Diagrams. Balkema, Rotterdam, pp. 1–18.
Walker, M., Head, M.J., Berkelhammer, M., Bjorck, S., Cheng, H., et al., 2019. Subdividing the Holocene Series/Epoch: formalization of stages/ages and subseries/subepochs, and designation of GSSPs and auxiliary stratotypes. Quat. Sci. Rev. 34, 173–186.
Wilson, J.L., Everard, M., 2017. Real-time consequences of riparian cattle trampling for mobilisation of sediment, nutrients and bacteria in a British lowland river. Int. J. River Basin Manage. 1–37.
WRB, IUSS Working Group, 2015. World Reference Base for Soil Resources 2014, update 2015. International soil classification system for naming soils and creating legends for soil maps. World Soil Resources Reports No. 106. FAO, Rome 2015.
Zoller, H., Schindler, C., Roethlisberger, H., 1966. Postglaziale Gletscherstaende und Klimaschwankungen im Gotthardmassiv und Vorderrheingebiet. Verh. Naturforsch. Ges. Basel 77 (2), 97–164.

Supplementary Fig. S1

Bergamo, ancient hilltop city, *Piazzetta Luigi Angelini*. Outcrop of limestone belonging to the Missaglia Megabed, Flysch di Bergamo formation. The pictured outcrop was presumably quarried at the time of the road construction, in the Roman Age.

Supplementary Fig. S2 – Plot of all available ages on calibration curve (Intcal 2013) to show the relationships of calibrated distributions with radiocarbon plateaux in the Bronze and Iron Ages.

https://c14.arch.ox.ac.uk/oxcal/ocp_plot_bw_svg.html

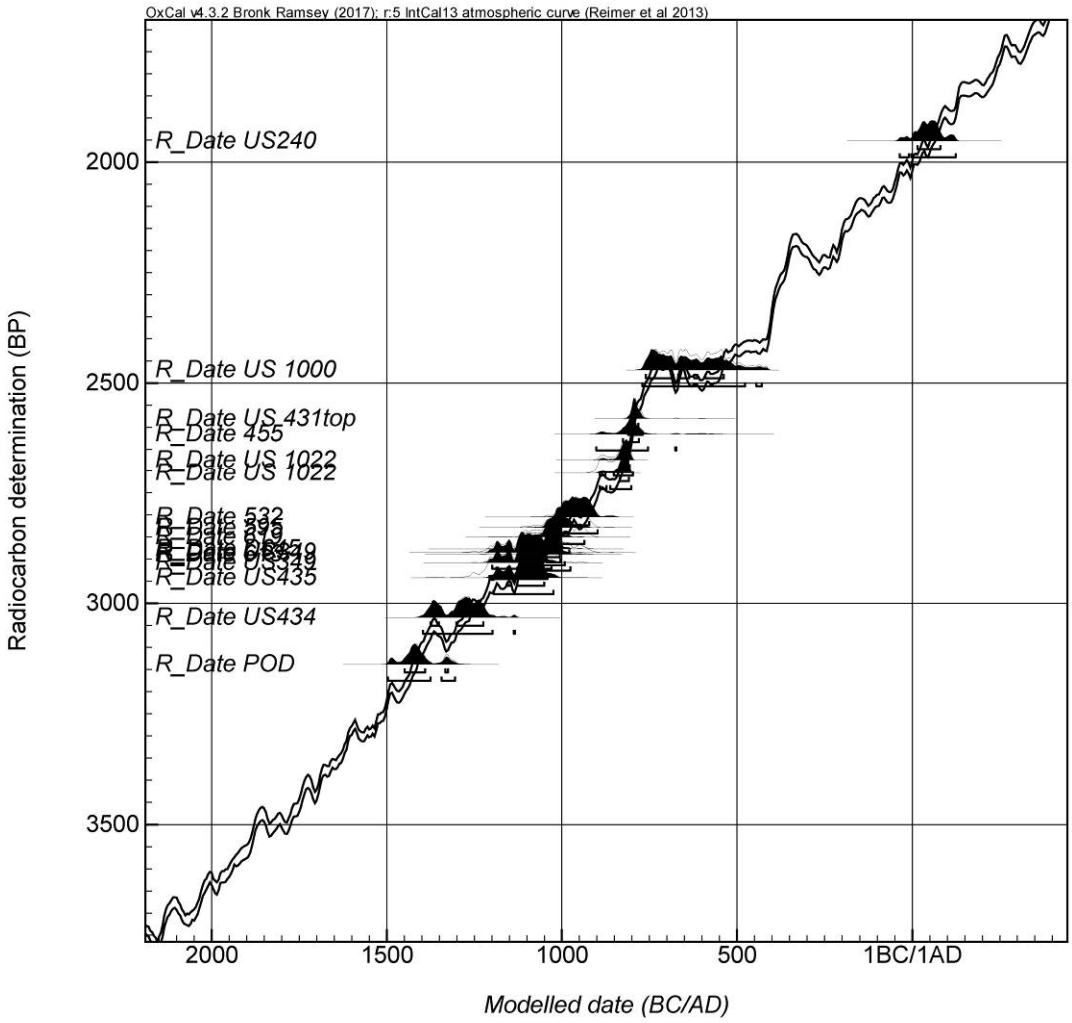

Supplementary Fig. S3 – Section A-B below the extant city viewed from NE showing the position of the main drillings beneath of the buildings. The section is traced in Fig. 3.

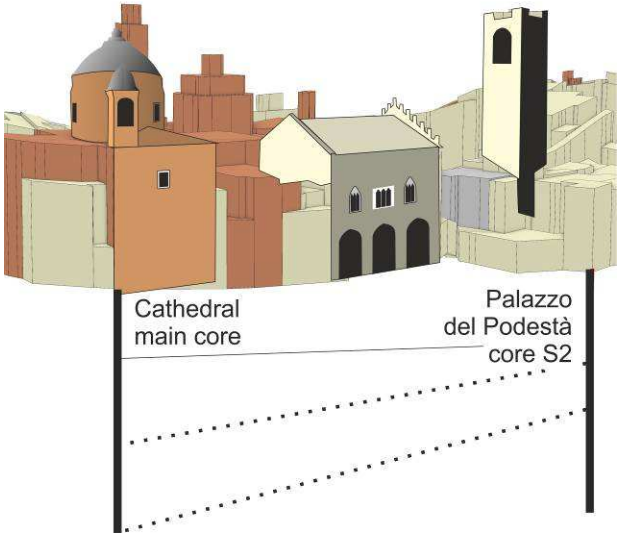

Supplementary Tab. S1

Site elevation data catalogue.

Site number in figures	Source of information	Site name	elevation (m asl)	bedrock elevation (m asl)	difference in elevation (m)	longitude (WGS84 UTM 32N)	latitude (WGS84 UTM 32N)
1	CNR, unpublished data	Cathedral main core	366	355,6	10.4	551627,2002	5061306,631
2	CNR, unpublished data	Cathedral trench C	366	359,8	6.2	551599,2008	5061304,631
3	Pini et al., 2016	Domus Bragagnoli trench C	366,5			551544,3055	5061370,021
4	CNR, unpublished data	Palazzo del Podestà, core S2	365,7	355,9	9.8	551570,1361	5061386,225
5	Lanza, 2003	LZ 1	369,5	368	1.5	551502,202	5061449,628
6	Lanza, 2003	LZ 2	367,5	369	1.5	551511,202	5061409,629
7	Lanza, 2003	LZ 3	365,5	363	2.5	551579,2007	5061404,629
8	Lanza, 2003	LZ 4	365	361	4	551606,2003	5061386,629
9	Lanza, 2003	LZ 5	364,5	361	3.5	551616,2	5061405,629
10	Lanza, 2003	LZ 6	361,5	352	9.5	551646,1993	5061443,629
11	Lanza, 2003	LZ 7	363	361	2	551649,5067	5061408,322
12	Lanza, 2003	LZ 8	357	337	20	551725,1978	5061454,629
13	Lanza, 2003	LZ 9	359	349	10	551713,1983	5061376,63
14	Lanza, 2003	LZ 10	359,5	352	7.5	551693,1987	5061371,63
15	Lanza, 2003	LZ 11	359,5	354	5.5	551695,1987	5061373,63
16	Lanza, 2003	LZ 12	361	355	6	551670,1991	5061377,63
17	Lanza, 2003	LZ 13	361,5	358	3.5	551781,1969	5061404,63
18	Lanza, 2003	LZ 14	361	355,5	5.5	551675,1992	5061340,631
19	Lanza, 2003	LZ 15	361	355,5	5.5	551673,1992	5061346,63
20	Lanza, 2003	LZ 16	361	356	5	551669,1993	5061340,631
21	Lanza, 2003	LZ 17	362	357	5	551665,8452	5061338,043
22	Lanza, 2003	LZ 18	357,7	356,5	1.2	551785,2844	5061296,624
23	Lanza, 2003	LZ 19	355,8	355,8	0	551787,1973	5061285,632
24	Lanza, 2003	LZ 20	354,5	354,5	0	551778,7579	5061258,94
25	Lanza, 2003	LZ 21	356	356	0	551777,1976	5061263,632
26	Lanza, 2003	LZ 22	359,8	359	0.8	551741,1983	5061259,632
27	Lanza, 2003	LZ 23	369	368	1	551636,2003	5061234,632
28	Lanza, 2003	LZ 24	369	368	1	551603,2009	5061256,632
29	Lanza, 2003	LZ 25	366	364	2	551541,2019	5061297,631
30	Lanza, 2003	LZ 26	365,7	366	-0.3	551471,2033	5061264,631
31	Lanza, 2003	LZ 27	369,5	368,5	1	551569,2015	5061257,632
32	Lanza, 2003	LZ 28	368,5	365,5	3	551541,2021	5061251,632
33	Lanza, 2003	LZ 29	369	365,5	3.5	551538,2022	5061237,632
34	Lanza, 2003	LZ 30	370	366	4	551538,2022	5061231,632
35	Technical Report SO.GE.TEC 2	Palazzo del Podestà, core S1	365,8	360,3	5,6	551568,379	5061380,001
36	Technical Report SO.GE.TEC 2	Palazzo del Podestà, core S4	365,8	358,6	7,2	551569,5509	5061383,943
37	Technical Report SO.GE.TEC 2	Palazzo del Podestà, core S3	366	356,2	9,8	551561,4543	5061395,768

Supplementary Tab. S2

Volume susceptibility k values measured on subsamples from stratigraphic units composing a domestic dump of Early Iron Age, site Cathedral trench C.

sample name	measured material	κ 10-5 SI
SU 1022 strato	charcoal-rich sandy silt (midden)	78±21
SU 1022 strato	charcoal-rich sandy silt (midden)	58±10
SU 1022 strato	charcoal-rich sandy silt (midden)	54±7
SU 1022 basale	charcoal-rich sandy silt (midden)	57±26
SU 1022 basale	charcoal-rich sandy silt (midden)	40±2
SU 1000	charcoal-rich sandy silt (midden)	30±3
SU 1000	charcoal-rich sandy silt (midden)	54±15
SU 1000	charcoal-rich sandy silt (midden)	38±10
SU 1000	charcoal-rich sandy silt (midden)	53±1
SU 1000 basale	charcoal-rich sandy silt (midden)	81±6
SU 431 top (429N)	charcoal-rich sandy silt (midden)	27±14
SU 431 top (429N)	charcoal-rich sandy silt (midden)	26±3
SU 431 top (429N)	charcoal-rich sandy silt (midden)	28±17
SU 420A basale	charcoal-rich sandy silt (midden)	82±2
SU 1005 tronchi	charcoalified structures	9±5
SU 1005 tronchi	charcoalified structures	0
SU 429 SUD basale	charcoal-rich sandy silt (midden)	38±1
SU 429 SUD basale	charcoal-rich sandy silt (midden)	129±19
SU 429 SUD basale	charred wood	0
SU 429 SUD basale	centimeter-sized ceramic fragment (midden)	135±52
SU 1005	charcoal-rich sandy silt (midden)	41
SU 1005	nodule (midden)	35
SU 1005	charred wood (midden)	5±5
average values		78±11

Supplementary Tab. S3

Oxcal CQL2 code defining chronological model for the stratigraphic sequences dated in the ancient city of Bergamo.

```
Plot()
{
P_Sequence("POD",1)
{
Boundary();
R_Date("POD", 3138, 31)
{
z=771;
};
Boundary();
};
P_Sequence("DuomoC",0.01)
{
Boundary();
R_Date("D645", 2877, 29)
{
z=621;
};
R_Date("619", 2850, 30)
{
z=617;
};
R_Date("613", 2889, 30)
{
z=613;
};
R_Date("595", 2829, 29)
{
z=595;
};
R_Date("532", 2805, 27)
{
z=532;
};
R_Date("455", 2615, 42)
{
z=455;
};
Boundary();
};
P_Sequence("Domus B",0.01)
{
Boundary();
R_Date("US434", 3032, 29)
{
z=386;
};
R_Date("US349", 2908, 29)
{
z=317;
};
R_Date("US349", 2885, 47)
{
z=317;
};
R_Date("US435", 2942, 34)
{
z=310;
};
R_Date("US240", 1952, 30)
{
z=260;
};
Boundary();
};
P_Sequence("Saggio C",0.01)
{
Boundary();
R_Date("US 1022", 2705, 25)
{
z=130;
};
R_Date("US 1022", 2674, 27)
{
z=130;
};
R_Date("US 431top", 2580, 24)
{
z=125;
};
R_Date("US 1000", 2470, 27)
{
z=5;
};
Boundary();
};
};
```

Supplementary Tab. S4

Posterior statistics for the studied sequences.

	Unmodelled (BC/AD)									Modelled (BC/AD)									Indices A_{model}=108.4 $A_{overall}$=110.4			
Name	from	to	%	from	to	%	μ	σ	m	from	to	%	from	to	%	μ	σ	m	A_{comb}	A	L	P C
R_Date US 1000	-751	-539	68.2	-768	-431	95.4	-624	87	-633	-761	-539	68.2	-771	-430	95.4	-635	90	-646		100.1		97.6
R_Date US 431top	-800	-778	68.2	-809	-761	95.4	-782	32	-789	-803	-783	68.2	-812	-770	95.4	-791	12	-793		97.3		97.1
R_Date US 1022	-841	-803	68.2	-895	-800	95.4	-834	26	-826	-834	-807	68.2	-892	-798	95.4	-826	19	-822		116.4		95.6
R_Date US 1022	-894	-818	68.2	-901	-811	95.4	-856	27	-853	-836	-809	68.2	-893	-802	95.4	-830	20	-825		97.8		95.7
▲ P_Sequence Cathedral Trench C																						
R_Date US240	16	80	68.2	-37	124	95.4	47	35	49	15	81	68.2	-37	125	95.4	48	36	49		98.1		98.8
R_Date US435	-1216	-1090	68.2	-1259	-1031	95.4	-1146	56	-1150	-1155	-1051	68.2	-1196	-1025	95.4	-1106	44	-1101		89.2		98.4
R_Date US349	-1188	-997	68.2	-1211	-931	95.4	-1070	72	-1068	-1155	-1054	68.2	-1200	-1031	95.4	-1110	44	-1105		107.5		98.6
R_Date US349	-1188	-1039	68.2	-1207	-1012	95.4	-1099	52	-1095	-1187	-1056	68.1	-1207	-1042	95.4	-1113	44	-1108		105.9		98.5
R_Date US434	-1375	-1229	68.2	-1397	-1208	95.4	-1292	55	-1284	-1376	-1225	68.2	-1397	-1135	95.4	-1290	58	-1282		97.5		99
▲ P_Sequence Domus dei Bragagnoli																						
R_Date 855	-822	-777	68.2	-897	-592	95.4	-792	54	-800	-826	-781	68.2	-902	-674	95.4	-803	46	-803		96.7		98.5
R_Date 932	-996	-922	68.2	-1042	-896	95.4	-957	36	-958	-992	-923	68.2	-1015	-899	95.4	-955	32	-956		103.3		99.6
R_Date 995	-1014	-930	68.2	-1071	-905	95.4	-982	42	-981	-1037	-982	68.2	-1052	-937	95.4	-1004	29	-1007		97.4		98.5
R_Date 1013	-1113	-1020	68.2	-1195	-977	95.4	-1073	52	-1070	-1044	-1005	68.2	-1093	-977	95.4	-1027	25	-1024		97.9		96.6
R_Date 1017	-1051	-941	68.2	-1111	-927	95.4	-1012	50	-1011	-1047	-1007	68.2	-1094	-980	95.4	-1030	25	-1027		120.2		96.2
R_Date 1021	-1110	-1009	68.2	-1190	-938	95.3	-1055	50	-1052	-1050	-1006	68.2	-1110	-993	95.4	-1034	27	-1030		120.3		95.4
▲ P_Sequence Cathedral main core																						
R_Date POD	-1448	-1323	68.2	-1497	-1304	95.4	-1405	48	-1415	-1450	-1326	68.2	-1498	-1306	95.4	-1411	46	-1418		100.3		99.2
▲ P_Sequence Palazzo del Podestà																						